FETAL ECG EXTRACTION USING NONLINEAR NOISE REDUCTION AND BLIND SOURCE SEPARATION

FETAL ECG EXTRACTION USING NONLINEAR NOISE REDUCTION AND BLIND SOURCE SEPARATION

BY
SHINGO YUKI, B.A.Sc.

A Thesis Submitted to
the School of Graduate Studies
in Partial Fulfillment of the Requirements
for the Degree
Master of Engineering

McMaster University

Master of Engineering (2002)
(Electrical and Computer Engineering)

McMaster University
Hamilton, Ontario

TITLE:	Fetal ECG Extraction
AUTHOR:	Shingo Yuki, B.A.Sc. (University of Waterloo)
SUPERVISOR:	Dr. Markad Kamath, Ph.D.
NUMBER OF PAGES:	clxi, 84

Abstract

The fetal electrocardiogram contains within it, information regarding the health of the fetus. Currently, fetal ECG is recorded directly from the scalp of the baby during labour. However, it has been shown that fetal ECG can also be measured using surface electrodes attached to a pregnant mother's abdomen. The advantage of this method lies in the fact that fetal ECG can be measured noninvasively before the onset of labour. The difficulty lies in isolating the fetal ECG from extraneous signals that are simultaneously recorded with it.

Several signal processing methodologies have been put forth in order to extract the fetal ECG component from a mixture of signals. Two recent techniques that have been put forth include a scheme that has previously been used to nonlinearly reduce noise in deterministically chaotic noise and the other uses a blind source separation technique called independent component analysis.

In this thesis, we describe the significance of the fetal electrocardiogram as a diagnostic tool in medicine, a brief overview of the theory behind the nonlinear noise reduction technique and blind source separation, and results from having processed synthetic and real data using both techniques. We find that although the noise reduction technique performs adequately, the blind source separation process performs faster and more robustly against similar data. The two techniques can be used in tandem to arrive at an approximate fetal ECG signal, which can be further analyzed by calculating, for example, the fetal heart rate.

DEDICATION

Cette thèse est dédiée à Lucille,
ma meilluere amie et l' allégresse de ma vie

Acknowledgements

This thesis is made possible with the generous aid and support of numerous individuals and groups to whom I owe a great debt.

First and foremost, I would like to thank Dr. Markad Kamath for his patience, guidance, and wisdom throughout this thesis. Thanks also to Dr. Barbara Brennan, the other principal investigator, for finding time in her busy schedule to follow through with this ambitious project.

I would like to express my appreciation to Dr. Patrick Mohide, Dr. S. Effer, Dr. Paul Kantor, Ms. Nancy Brown, R.N., Ms. Hazel Baird, R.N., and Elaine Moore, R.N., who all shared their precious time and energy to provide me with their insights, ideas, and skills, allowing me to navigate otherwise frightening waters. Thanks in particular to Nancy, Hazel, and Elaine for being there with me during the recording sessions, and ostensibly keeping in touch with me with regards to available volunteers.

I am extremely grateful to all of our volunteers. The data we collected with their assistance and cooperation is invaluable. Thank you to them and their generous spirits.

I am deeply indebted to Cheryl Gies, the Graduate Secretary of the Department of Electrical and Computer Engineering at McMaster University. I wish to acknowledge my gratitude for your timely help on countless occasions.

On a personal note, I would like to thank Justine for giving me, in her smile and laughter, that little bit of energy I needed to step out the door in the morning and come to work on campus, especially during the summer months. I'd also like to thank Martyn for bringing beautiful sculpture into the house so that once in a while I could stop being an engineer and contemplate art.

Finally, I am grateful to Dr. Upton and the DeGroote Foundation for providing the necessary computers and laboratory facilities to complete this thesis, and the Natural Science and Engineering Research Council of Canada who provided research funding.

TABLE OF CONTENTS

List of Figures

List of Tables

Glossary

Auscultation	The act of listening for sounds within the body, chiefly for ascertaining the condition of the lungs, heart, pleura, abdomen and other organs and for the detection of pregnancy.
Antepartum	Before labour or childbirth.
Bradycardia	A slowness of the heart beat, as evidenced by slowing of the pulse rate to less than 60 beats per minute.
Cerebral Palsy	A persisting qualitative motor disorder appearing before the age of three years, due to non-progressive damage to the brain.
Cutaneous	Pertaining to the skin, dermal, dermic.
Fundus	The bottom or base of any hollow organ; as, the fundus of the bladder; the fundus of the eye.
Fundic	Pertaining to the fundus
Hypoxaemia	The reduction of the oxygen concentration in the arterial blood, recognized clinically by the presence of central and peripheral cyanosis. When the partial pressure of oxygen (pO2) falls below 8.0 kPa (60 mmHg), the condition is defined as respiratory failure.
Hypoxia	Reduction of oxygen supply to tissue below physiological levels despite adequate perfusion of the tissue by blood.
Intrapartum	During labour and delivery or childbirth.
Intrauterine	In the uterus (the womb).
Noninvasive	Denoting a procedure that does not require insertion of an instrument or device through the skin or a body orifice for diagnosis or treatment.
Supine	Lying on the back.
Tachycardia	The excessive rapidity in the action of the heart, the term is usually applied to a heart rate above 100 per minute and may be qualified as atrial, junctional (nodal) or ventricular and as paroxysmal.

List of Abbreviations

ACF	Autocorrelation function
BSS	Blind source separation
CMRR	Common mode rejection ratio
FECG	Fetal Electrocardiogram
FHR	Fetal heart rate
ICA	Independent component analysis
MECG	Maternal electrocardiogram
NLNR	Nonlinear noise reduction
SNR	Signal to noise ratio
SNR_{MF}	Signal to noise ratio between MECG-FECG
SVD	Singular value decomposition
UPI	Utero-placental insufficiency

Chapter 1

Fetal Monitoring and Fetal Electrocardiography

1.1 INTRODUCTION

Often it is necessary to monitor the heart condition of a fetus during pregnancy in order to assess health and diagnose possible diseases. This is especially true for high-risk pregnancies where it is necessary for the physician to know about the existence of fetal distress syndromes, which indicate problems in fetal oxygenation. For humans, prolonged periods of oxygen deprivation results in a variety of brain injuries. In the case of the fetus, there is the possibility of permanent damage to the brain and nervous system, which, for example, may manifest itself in the form of cerebral palsy. Early detection and diagnosis helps increase the effectiveness of any appropriate intervention. Therefore, it remains relevant to continuously investigate the possibility of finding indicators of disease as early as possible during pregnancy. Valuable clinical information can be

obtained by performing an antepartum analysis of the condition of a fetus. Although there are some commercial tools available for the intrapartum recording of the fetal electrocardiogram (FECG) via scalp electrodes used during labour, there is still little available to the physician in the way of off-the-shelf tools to aid the obstetrician before the onset of labour. Recent literature by Zarzoso and Nandi (2001), DeLathlauwer et al. (2000), Richter, Schreiber and Kaplan (1996), and Kanjilal et al. (1997), suggests that there are methodologies that engineers can effectively use to assist the obstetrician to non-invasively and reliably obtain and analyze the FECG. The objectives of this thesis are as follows

A. To develop a hardware/software for recording and extracting the fetal electrocardiogram from abdominal recordings.

B. To make a series of local recordings to and document the performance of our system.

The first chapter gives an overview of fetal physiology, the medical motivation for obtaining information regarding the fetus (especially the FECG), and the development of fetal electrocardiography over the last 50 years. The first chapter also discusses the engineering efforts that have been made to extract fetal heart information from mixed abdominal electrode recordings. The second chapter of the thesis describes the theory of nonlinear noise reduction (NLNR) and blind source separation (BSS) – two techniques that we employ and will be compared for the extraction of the fetal heart signal from the mixed abdominal recordings. The third chapter outlines some design considerations pertaining to the data acquisition hardware and the recording protocol. The thesis

concludes with a summary of findings of the studies using our analysis tools on abdominal recordings both obtained from other centers and data recorded locally.

1.2 FETAL ELECTROCARDIOGRAMS

1.2.1 Fetal Physiology

Consider the simplified diagram of the fetal circulation depicted in Figure 1.1. The placenta is the organ inside the uterus that functions as the exchange station for chemicals including water, oxygen, nutrients, and waste chemicals (e.g. carbon dioxide). These chemicals collectively exist in the form of amniotic fluid on the fetal side of the placenta while the same chemicals are carried to and from the placenta via arteries and veins on the maternal side. Clearly, changes in the uterine blood flow will affect the manner in which the fetus exchanges vital chemicals. Physicians are aware of several factors that cause a decrease in uterine blood flow. For example, the flow through the intervillous space may decrease due to position, exercise, uterine contractions, maternal hypertension, or anesthesia. In the present context, we are particularly interested in the effects of any such decrease in uterine blood flow on the amount of oxygen received by the fetus, (fetal oxygenation). A primary concern for obstetricians is fetal hypoxia – a condition that can result from a prolonged decrease in uterine blood flow. Such a state is known as utero-placental insufficiency (UPI). Chronic UPI may be associated with intrauterine growth restriction and/or antepartum fetal death (Freeman, 1991).

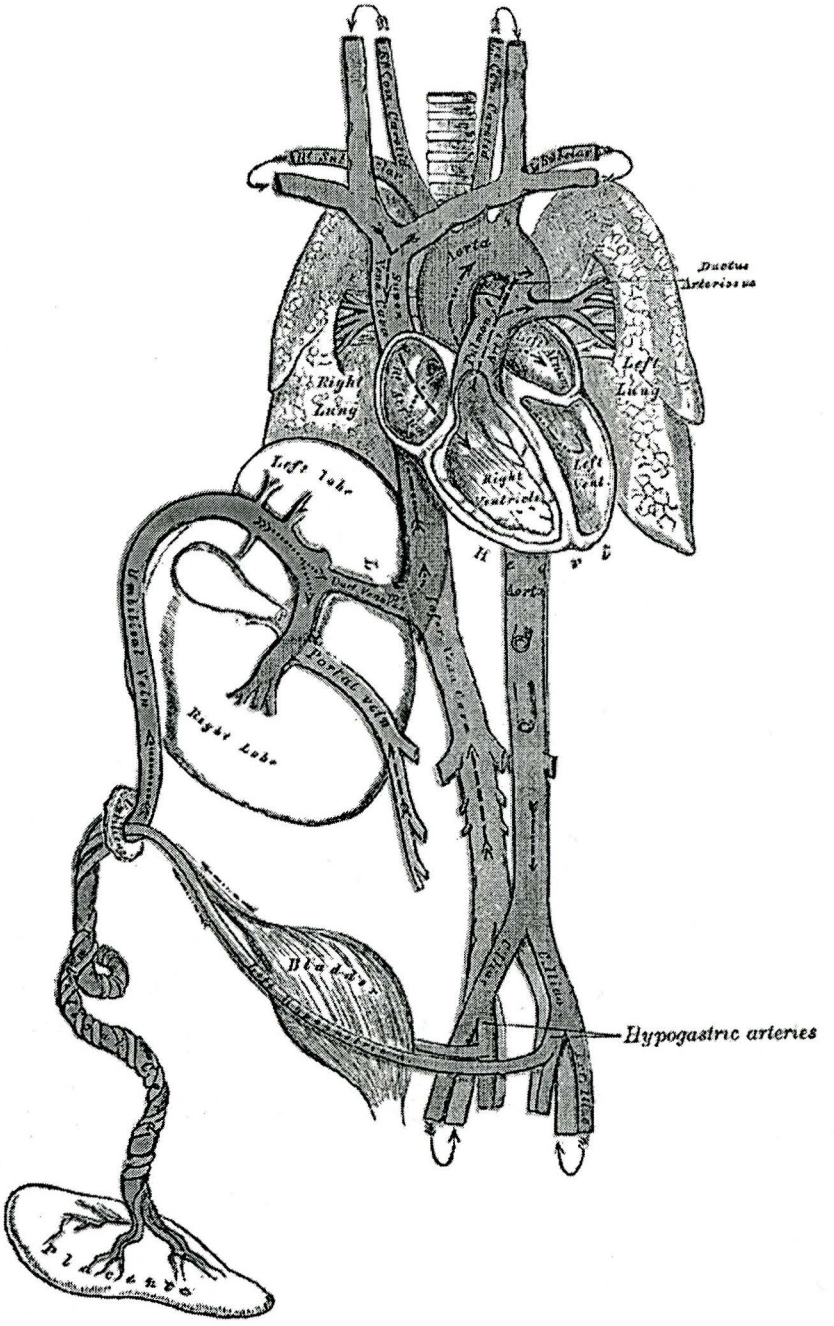

Figure 1.1 Fetus-placenta model. Note that the well-oxygenated blood returning from the placenta via the inferior vena cava (IVC) crosses into the left atrium while the superior vena cava (SVC) blood tends to run into the right ventricle. The placenta is connected to the fetus (not shown here) and resides inside the uterus. (Source: http://www.bartleby.com/107/Images/large/image502.gif)

1.2.2 Clinical Significance of FECG Morphology

The FECG is closely related to the adult ECG, containing the same basic waveforms including the P-wave, the QRS complex, and the T-wave. The PR Interval reflects the conduction time in the AV node and the QRS complex represents ventricular depolarization. The FECG directly displays the muscle particular shapes of the FECG waveform that can serve as direct evidence of specific malfunctions and abnormalities. Morphologies of interest include the shape, size, and duration of individual and groups of FECG waveforms as well as the various ratios relating these quantities to each other. Table 1.1 summarizes some of the FECG waveform-based quantities that have been linked to particular physiological phenomena.

WAVEFORM	PHYSIOLOGICAL INTERPRETATION AND SIGNIFICANCE	SOURCE
PR Interval	PQ interval is prolonged in the asphyxiated fetus	Pardi and Croignani, 1971
PR/FHR Ratio	Positive PR/FHR correlation and shortening of PR interval for fetal compromise and hypoxaemia	Murray, 1986
T/QRS Ratio	Strong correlation with rate of rise of lactate	Greene et al., 1982
ST Segment	Biphasic ST segment associated with myocardial hypoxia	Rosen, 1976

Table 1.1 Physiological Interpretations of Various FECG Waveforms

1.2.3 Clinical Significance of Fetal Heart Rate

Monitoring of the fetal heart rate gives an indirect measure of the fetal state through an understanding of the physiological conditions and mechanisms that give rise to changes in the heart rate. To this end, this section briefly illustrates the meaning behind the fetal heart rate in terms of the physiological state of the fetus.

As is the case with adults, the heart rate variability of a developed fetus is dependent upon its own autonomic nervous system. Accelerations of the heart rate (tachycardia) are precipitated by signals sent via the sympathetic nerves and decelerations (bradycardia) sent via the vagal nerve (sometimes referred to as parasympathetic stimulation). The only other immediate factor governing the heart rate would be the atrial pacemaker node found on the heart itself. Therefore, marked accelerations and decelerations can be traced to particular factors that influence the sympathetic and parasympathetic nervous system. For example, stimulation of baroreceptors in the aortic arch (through changes in blood pressure) and chemoreceptors in the cartoid sinus (through changes in partial oxygen pressures or "pO_2") both result in a deceleration mediated by the vagal nerve. In the case of a fetus under normal circumstances, the heart rate ranges from 120 to 160 beats per minute (bpm) (Symmonds, 2001).

Barcroft initially showed results that indicated a link between umbilical cord occlusion, a parasympathetic response, and significant decelerations in FHR (Barcroft, 1947). Umbilical occlusion initiates an increase in fetal blood pressure (categorized as fetal hypertension) resulting in the stimulation of fetal baroreceptors, which leads to a central vagal response and a subsequent deceleration in FHR. Further work by Siassi also illustrated how changes in arterial pO_2 also contributed to this reflex bradycardia. Incidentally, intermittent hypoxia was found not to result only in vagally influenced bradycardia but prolonged hypoxia was found to cause metabolic acidosis, which lead to myocardial depression – a secondary mechanism for causing decelerations (Siassi, 1973).

Thus, it is believed that FHR decelerations are an indicator of a decrease in the flow of oxygenated blood to the fetus and/or some fetal hypoxemic episode that is

limiting the amount of oxygen received by the fetus (Freeman, 1991). The mechanism linking fetal oxygenation and decelerations in the fetal heart rate is summarized in Figure 1.2.

1.3 EVOLUTION OF FETAL ELECTROCARDIOGRAMS

1.3.1 A Brief History of Fetal Electrocardiography

Cremer performed the first documented recording of a fetus' heart signal in 1906. Over the next 50 years, various improvements to fetal electrocardiography were made in the way of amplification, and abdominal electrode placement, mostly in an attempt to improve resolution of the fetal QRS complex and calculate the fetal heart rate (FHR). Often, such efforts resulted in the complete obliteration of the P and T waves (Symmonds, 2001). In the mid-1950's the introduction of intrauterine electrodes (i.e. electrodes placed on the scalp of the baby via the birth canal during labour) and improved filtering techniques allowed physicians to obtain P and T waveforms whose shapes and positions they could relate to various fetal characteristics such as oxygen saturation and bradycardia (Symmonds, 2001). Thereafter, many of the advances in improving the signal quality of the FECG focused on signals acquired directly from the fetus during the birthing process. The series of papers published by Hon and Lee on fetal electrocardiography from the early 1960's, for example, still dealt primarily with recordings from scalp electrodes. Improvements to signal-to-noise ratio that Hon and Lee discuss in their papers focused primarily on triggered averaging used in combination with analog filters (Hon and Lee, 1963). The use of scalp electrodes remains common as

is evidenced by the design of fetal monitors that are available from major medical equipment manufacturers such as GE Medical and Hewlett Packard.

1.3.2 FECG Extraction from Abdominal Recordings

Initially, isolation of the FECG from the maternal abdominal recording containing both the FECG and the maternal electrocardiogram (MECG) was implemented with fairly elementary methods. These methods focused on the subtraction of the MECG from the mixed FECG-MECG abdominal recordings. In some cases (e.g. Surreau, 1955 and Wheeler, 1978), a separate MECG was recorded from the mother's chest in addition to the abdominal recordings. These schemes generally involved the "elimination" (whether through matched amplitude subtraction or outright erasure) of the MECG from the mixed abdominal signal. A major drawback of these methods was the difficulty of matching the MECG patterns in the abdominal recordings with those recorded from the chest region.

In 1966, Van Bemmel published a pioneering procedure based on statistical signal processing for detecting the FHR (Bemmel, 1966). His particular scheme was less of a separation method than a technique to detect the presence of a fetal heart beat and estimate the FHR based on a windowed (i.e. using finite segments of an ECG signal) autocorrelation function (ACF). Van Bemmel compared the ACF of a mixed abdominal signal and that of some reference signal containing only the MECG (how this was obtained remains unspecified). There was a notable discrepancy between the two ACF's at a particular lag time that corresponded with the average fetal heart rate (Bemmel, 1966). Autocorrelation is still used to determine short-term fetal heart rate using

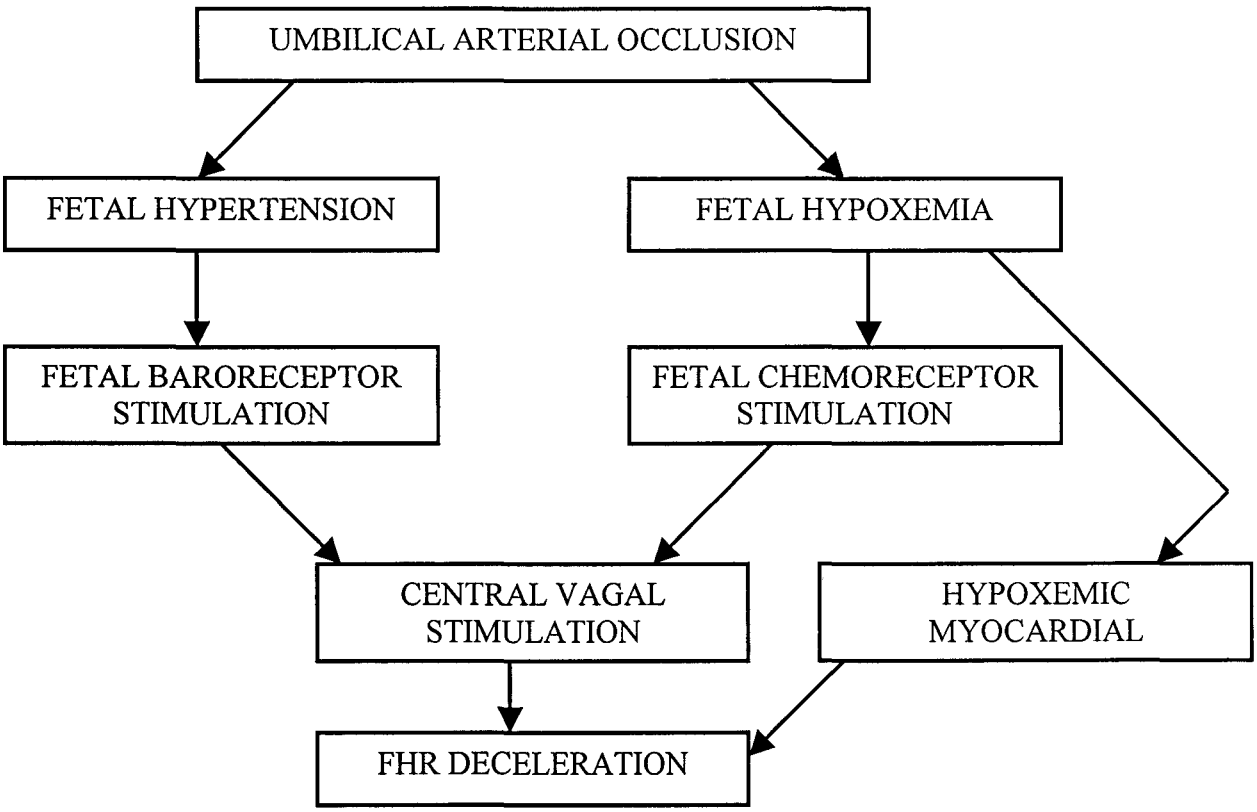

Figure 1.2 Mechanism for decelerations in FHR (Source: Freeeman, (1991))

ultrasound signals (Peters, 1990). Since Van Bemmel's method was published in an engineering journal it received very little exposure in the obstetrics community, which at the time was focused on the work of Hon and Lee.

Further progress was made in FECG extraction by Ferrara and Widrow (1982) who applied the idea of using a linear combination of multiple observations to achieve a the desired signal from a mixture of signals. Ferrara and Widrow's technique in particular uses the now-familiar adaptive signal enhancement model where the error between some reference signal and a linear sum of multiple signals is minimized through the adaptation of tap weights (Ferrara and Widrow, 1982). In a similar concept, Bergveld and Meijer (1981) published a paper that forwarded the idea of arriving at an optimal linear combination not by adaptive noise cancellation but through a type of "spatial filtering". Although their work did not result in total signal separation, their idea that electrode position need only be adjusted for maximum FECG amplitude and was not considered critical for the actual separation process was significant (i.e. electrode position is accounted for in the optimization of the weights).

Vanderschoot and Callaerts built on the ideas of Bergveld and Meijer (1981) by applying singular value decomposition (SVD) to the multiple samples of multiple electrode recordings. By doing so, they argued that orthogonality was the key to maximally separating the physiological signals found in the mixed abdominal recordings. Specifically, their work used, as a starting point, the assumption that FECG and MECG were orthogonal in signals space as well as the columns of the transfer vector. Although their assumptions did not quite match with recorded data, good signal separation was achieved, especially with the incorporation of thoracic MECG recordings, which aided in

the differentiation between FECG and MECG in signal space (Vanderschoot and Callaerts, 1987). Kanjilal et al. suggested that SVD could be performed on a single channel recording to extract FECG by building an observation matrix of consecutive samples of a single recording. The separation resulting from the method outlined by Kanjilal et al. (1997) appears good although the implementation of an automated scheme of building the observation matrix based on a singular value ratio (SVR) spectrum remains unclear (Kanjilal, 1997).

In 2000, De Lathauwer et al. presented a method to extract the FECG using blind source separation (BSS) (DeLathauwer et al., 2000). The use of BSS techniques on abdominal signals retained the idea of linearly combining the multiple ECG signals but differed in the criterion used in arriving at an optimal set of weights. Here, the driving force behind the optimization was the idea of making the resulting combined signals as statistically independent from each other as possible. One interesting aspect of using the BSS model for FECG extraction is the clear indication of the need to consider the statistical characteristics of the signals through the use of higher-order statistics whereas previous solutions attempted inversion using, at most, second-order statistics. DeLathauwer et al. (2000) also formally outlined how the FECG problem is essentially one that involves multiple sources (assumed to be independent), some unknown instantaneous mixture matrix that mixes these sources up (assumed to be linear), and multiple observations. This is of course the initial framework for a particular kind of BSS method known as independent component analysis (ICA). De Lathauwer et al. demonstrated the effectiveness of ICA on FECG isolation and their work was followed by a paper from Zardoso and Nandi (Zardoso and Nandi, 2001) comparing DeLathauwer

et. al's technique with adaptive weighting methods proposed by Callaerts et. al (Callaerts et al., 1990). Their comparisons show that the increased computational complexity of BSS methods resulted in a more robust approach.

While progress was being made in the domain of signal processing – largely a field within engineering – independent work was being made by some physicians collaborating with physicists who specialized in deterministically chaotic systems. This particular thread of work began with Schreiber and Kaplan's paper on noise reduction in ECG's (Schreiber and Kaplan, 1996), which was based on similar work on chaotic data (e.g. Henon and Ikeda maps) (Grassberger et al., 1993).

1.4 SUMMARY

The fetal electrocardiogram is useful in diagnosing the health of a fetus by it s morphology as well as its derivative quantities such as fetal heart rate. Although there is now a good understanding of how to interpret the fetal electrocardiogram, the actual acquisition of the signal remains a challenge. A variety of signal processing techniques have been proposed that address the extraction of the antepartum FECG from skin electrodes attached to the abdomen of pregnant women.

Chapter 2

FECG Extraction – Signal Processing Theory

2.1 OVERVIEW

Outside of instrumentation issues, the main focus of this thesis is related to the mathematical aspects of the feta electrocardiogram (FECG) extraction process. This chapter describes the theoretical basis for the two techniques we have chosen to use: nonlinear noise reduction and blind source separation. The principles of both techniques are examined, after which the application specific details of these techniques with regards to FECG extraction will be presented. The framework for nonlinear noise reduction involves the idea of delay space representation as well as the primary parameters that affect this representation: embedding window length and nearest neighbourhood size. Blind source separation separates signals by maximizing their respective independence in a statistical sense. Although the descriptions contained within are often mathematical,

this chapter is meant to an intuitive idea of how both techniques are able to separate the FECG from an otherwise mixed signal.

2.2 NONLINEAR NOISE REDUCTION (NLNR)

Quasi-periodic signals are accessible to a unique noise reduction approach. Unlike aperiodic signals, quasi-periodic signals have repeating patterns in time even though the patterns themselves may be completely irregular and the period may show significant variation. The noise reduction scheme involves:

1. Transforming the data into its delay space representation
2. Making lower-dimensional linear approximations of short segments of the transformed data
3. Projecting individual data points onto the lower-dimensional subspace associated with the linear approximation
4. Resolving all the corrections made to the transformed data and applying an inverse transform to arrive at a corrected time-series.

2.2.1 Delay Space Representation

Many systems do not lend themselves towards traditional linear filtering techniques such as Fourier-based filters that assume that a distinction between noise and signal can be found in frequency space. For such systems, an alternate approach to capturing the characteristics of a signal involves breaking down the signal into a series of delay vectors. For a given moment in time t, each delay vector contains values of the time series x at t, $t-\tau,...,t-(m-1)\tau$ where m is some positive integer and τ is a real-valued

delay interval. Each delay vector represents a co-ordinate in an m-dimensional delay space (sometimes called phase space or an embedding space) and the delay co-ordinates form what is known as an attractor - a pattern resembling a closed loop around which delay co-ordinates are scattered possibly due to non-stationarity and noise.

In order to construct a "good" delay space representation of the signal, it is necessary to determine an m and a τ that adequately capture the characteristic attractor. In nonlinear time series literature, the parameters m and τ are collectively called the embedding and there have been several embedding theorems put forth that attempt to quantitatively arrive at appropriate embedding lengths (Grassberger, 1994). The alternative is to use heuristic approaches that require careful observation of the characteristic temporal patterns and a series of visualizations of lower dimensional delay representations. Appropriate plots used in an explorative way can actually prove useful in exploiting the structure hidden in scalar time series (Grassberger, 1994). Figure 2.1 demonstrates how different characteristic components of an ECG waveform are represented in a two-dimensional delay space (i.e. $m = 2$) with $\tau = 0.02$ seconds.

2.2.2 Correction by Local Linear Approximation in Delay Space

The principle of the noise reduction scheme lies in projecting delay vector co-ordinates onto a local linear approximation of the attractor surface. The linear approximation consists of a subspace defined by the principal components of a local cluster of points in delay space. Consider, for example, a time signal of length T seconds that has been converted into a delay space representation for a particular m and τ. For simplicity let $\tau = nk$ where n is some positive integer and k is the sampling rate. The

resulting data set consists of a total of $Tk-(m-1)\tau$ m-length delay vectors. The correction of any particular delay vector x begins by searching the data set for its nearest neighbours according to, say, some Euclidean distance. In practice, this process should be limited to a reasonably sized subset of the data in order to speed up the overall process. In addition, the nearest neighbourhood's size could be increased to incorporate a minimum number of neighbours (Schreiber and Kaplan, 1996). For example, we could design our algorithm so that the initial Euclidean distance is increased by 10% until some minimum number of neighbours is found. Once a suitable neighbourhood is determined, the eigenvectors and eigenvalues for that neighbourhood are computed. The eigenvectors associated with the largest p eigenvalues (where $p<m$) are considered to span the subspace that is representative of the enveloping ellipsoid of the delay co-ordinates. The delay vector x is then "corrected" through an orthogonal projection onto this subspace. This correction procedure is repeated for all points in the transformed data set.

2.2.3 Reconstruction

Once the correction scheme is completed for all vectors, they need to be recombined into a single time-series. Since each element of the scalar time series is a member of m different but consecutive delay vectors, it is necessary to find the average of these m different "instances" of a particular time-series element when performing reconstruction. Consequently, a delay vector set created from the reconstructed time series would actually not lie precisely on the local subspaces but are moved toward them (Schreiber and Kaplan, 1996).

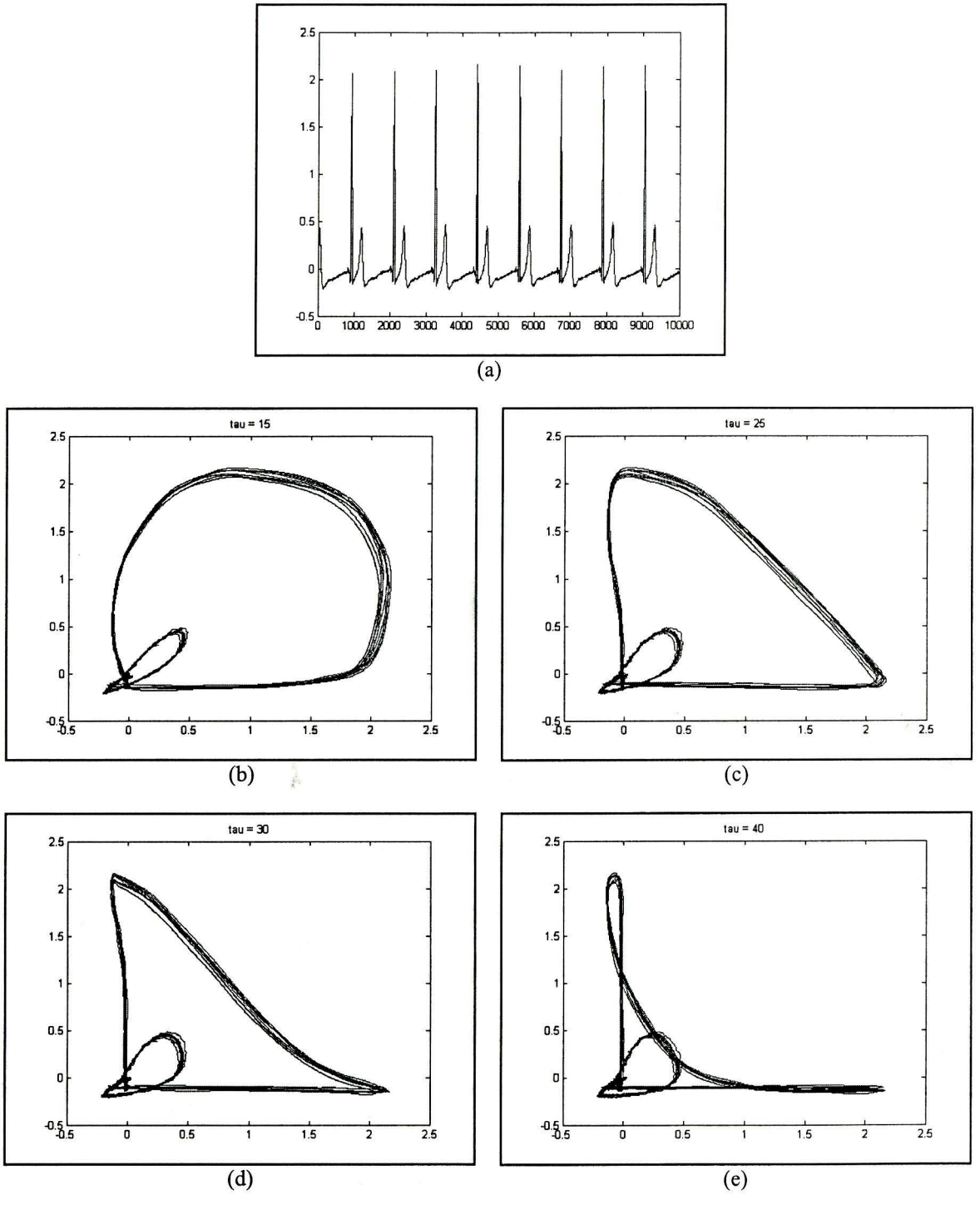

Figure 2.1 Two-dimensional delay space representation of ECG. (a) Original ECG sample, which is relatively noise free (b)-(d) Two-dimensional plot of delay space co-ordinates which are spaced apart by various tau values. Actual temporal spacing is tau multiplied by the sampling interval (2 ms in this case). The large loop represents the QRS complexes while the P and T waves reside in the smaller loop. Note that particular tau values directly affect the ambiguity of what the delay co-ordinate represents in the original time series.

2.3 BLIND SOURCE SEPARATION

Consider the classical example of a recording a conversation between multiple people in an echoless room using five microphones in varied positions around them. Each of the microphones records a (possibly) unique combination of the conversation depending on its relative proximity to the various people. Using only the five recordings, we want to isolate, as much possible, each person's voice. Knowing next to nothing about the situation in the room makes the problem a "blind" source isolation or separation problem. However, the lack of prior information is, in some sense, compensated by the "statistically strong but often physically plausible assumption of independence between the source signals." (Cardoso, 1998) The idea is to find some way of mixing the observations (i.e. the recordings) such that the initial mixing process is "reversed". The criterion that drives this process of "remixing" the observations is some measure of statistical independence between the resulting "remixed" signals.

For non-engineers, the task of blindly separating two mixed signals may seem somewhat mysterious. Consider though the addition of multiple random variables from a statistical point of view. The Central Limit Theorem states that the sum of even two independent random variables is more Gaussian than the original variables, and thus as the number of summed independent random variables increases, the closer to Gaussian the distribution of that sum becomes. By constraining our sources to be non-Gaussian (except possibly for one source), separation becomes a process of finding the right weights that will allow the weighted sum of the observations to be maximally distributed in a non-Gaussian fashion. What we need then, from a high level perspective, is some measure of Gaussianity/non-Gaussianity for a given sampling of random variables (in

particular, the "remixture" of our observations). Many such measures have been suggested, from fourth-order statistics of a signal to information theoretic quantities such as negentropy. These ideas and will be more fully explored in the Section 2.2.3.

Briefly, the idea of blind source separation can be approached from different paths, and the equivalencies between these approaches have been shown by Hyvarinen (Hyvarinen et al., 2001). Here, we will constrain our explanation to two prominent interpretations of blind source separation: Maximum likelihood estimation and information theory. The development of BSS from these two frameworks essentially leads to a coherent picture of why blind source separation tends to work as well as arriving at a practical and popular BSS algorithm known as independent component analysis (ICA).

2.3.1 The BSS Model

Before proceeding with the various mathematical derivations, it is necessary to establish the premise for the particular kind of blind source separation that will be dealt with in subsequent sections. Specifically, we need to establish some fundamental conditions and assumptions:

2.3.2.1 Source Independence

The sources are assumed to be statistically independent. Consider two random vectors s_1 and s_2, which represent our source signals. Independence implies that information on s_1 does not yield any information about s_2. A strict mathematical

definition of independence requires introducing joint and marginal probability density functions (p.d.f.'s) for s_1 and s_2:

$p_{12}(s_1,s_2) \rightarrow$ joint p.d.f. of s_1 and s_2

$p_1(s_1) \rightarrow$ marginal p.d.f. of s_1 defined to be $\int p_{12}(s_1, s_2)d\, s_2$

$p_2(s_2) \rightarrow$ marginal p.d.f. of s_2 defined to be $\int p_{12}(s_1, s_2)ds_1$

Given these defined quantities, our source signals s_1 and s_2 are said to be statistically independent if and only if

$$p_{12}(s_1,s_2) = p_1(s_1)p_2(s_2) \qquad \textbf{(2.1)}$$

Similarly, for a set of n random vectors to be independent, their joint probability density function would have to be the product of their respective marginal densities.

2.3.1.2 Limits on the Number of Gaussian Sources

One fundamental constraint in ICA is that, at most, only one of the sources can be distributed in a Gaussian fashion if ICA is to work. The rationale behind this restriction can be best explained by examining a multivariate distribution of two Gaussian random variables with identical variances that has been decorrelated (rotated). The resulting joint distribution is completely symmetrical and ambiguous (Figure 2.2a). Contrast this with, for example, a similar example with the Gaussian densities replaced by uniform densities. In this case, the existence of different components is unambiguous (Figure 2.2b). The asymmetry in the joint density would clearly be visible even if one of the two random variables had a Gaussian distribution.

2.3.1.3 Mixing

The methods to be explored here are for use when the signal mixture can be assumed to be instantaneous, without delays and echoes. Such complications would require moving away from an additive mixture to a convolutive mixture, which requires slightly different separation criteria. ICA algorithms do not inherently account for convolutive mixing and therefore their application would not be appropriate for such cases. In addition, we would ideally like some statistical stationarity in the mixing process. That is, the mixing process does not drastically change from moment to moment. Strictly speaking, this is not a necessary condition although the rate of change of the mixing process will affect the ability of our algorithm to converge to a particular "remixture" solution.

The most basic BSS model has n independent signals $s_1(t),...,s_n(t)$ denoted by an n-dimensional vector s(t) and the observations $x_1(t),...,x_m(t)$ denoted by x(t). Ideally, we have $m \geq n$ (i.e. an equal number or more observations than sources) defined in one of two ways:

$$x_i(t) = \sum_{j=1}^{n} a_{ij} s_j(t) \tag{2.2}$$

$$x(t) = As(t) \tag{2.3}$$

A is the unknown m x n mixing matrix that has rows that correspond to the n-length weight vector a_{ij}. As mentioned in section 2.1, we want to somehow combine our observations (i.e. the individual elements $x_i(t)$) to arrive at out source approximations $y_1(t),...,y_n(t)$ or y(t). Given a "remixing" matrix W, we can write

$$y(t) = Wx(t) \rightarrow y(t) = BAs(t) = Zs(t) \tag{2.4}$$

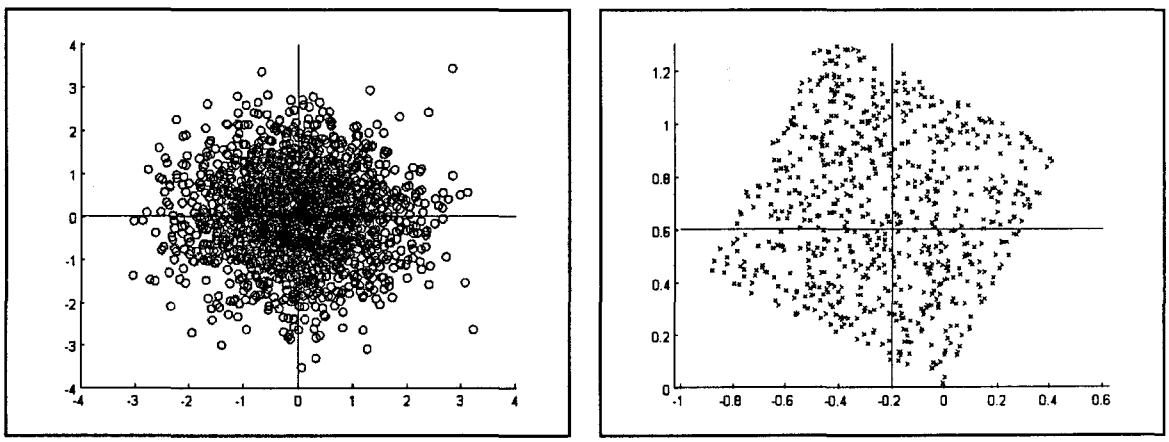

(a) (b)

Figure 2.2 (a) A multivariate distribution of two independent Gaussian variables. The orientation of each component is unclear. (b)A joint distribution of two independent variables distributed uniformly. Note that the direction of each component is unambiguous, in contrast to the two independent Gaussian variables

Note that y(t) can easily be interpreted as a linear combination of the source vectors. W is an n x m matrix that is found adaptively according to some criterion of convergence. Criteria are often summarized in the form of functions known as a cost or contrast functions and convergence is a matter of optimizing such a function. A brief exploration of the nature of source separation gives a better idea of appropriate/practical cost functions.

2.3.2 Maximum Likelihood Estimation

For a given data model, "likelihood" is the probability of obtaining a certain data set as a function of the parameters of that model (Cardoso, 1998). This gives us a way of watching how the changes in parameters affect the chances of arriving at the observations that have been made. In fact, the goal becomes one of maximizing this likelihood and simultaneously finding the right parameters and the right models for the data. This is the idea behind maximum likelihood estimation (MLE). In the context of signal separation, a "model" refers to a statistical model that describes the way some quantity is distributed (e.g. a Gaussian model). In fact, the quantities in question are the source signals whose models are assumed to be unknown. We are, in essence, trying to "guess" and arrive at the model that best approximates the model describing the distribution of the source signals.

In this formulation, we will drop the time index on our signal vectors and simply denote the source, observation, and source approximation signals as s, x, and y respectively unless otherwise noted. In addition, the derivation assumes m = n or that there are an equal number of observations and sources, implying that A is a square

matrix. Suppose that the p.d.f. for s is q(s). The density of x = As conditioned on a particular A and q(•) (the probability distribution of s) is then given by Cardoso (1998) as:

$$p(x;A,q) = \left|\det A\right|^{-1} q\left(A^{-1}x\right) \tag{2.5}$$

This conditional probability is called the likelihood of x. The "A^{-1}" term is actually the remixing/demxing matrix that we intend to find as a part of our separation scheme. Hence, let us replace A^{-1} by W and write the absolute value of the determinant of A as a constant term c. Next, let us then define $X_{1:N}$ as the matrix whose N columns represent N successive but independent realizations of the vector x. We then have

$$p(X_{1:N};W,q) = \prod_{k=1}^{N} p\left(x(k);W,q\right) = \prod_{k=1}^{N} c^{-1} q\left(Wx(k)\right) \tag{2.6}$$

If we take the log of both sides and normalize each side by dividing by N, we get the normalized log-likelihood of seeing $X_{1:N}$:

$$\frac{1}{N}\log p(X_{1:N};W,q) = \frac{1}{N}\sum_{k=1}^{N}\log q\left(Wx(k)\right) + const. \tag{2.7}$$

As the number of realizations N approaches ∞, the left side of the equation approaches the expected value of the quantity in the summation and hence we get

$$\lim_{N\to\infty}\frac{1}{N}\sum_{k=1}^{N}\log q\left(Wx(k)\right) + const. = E\left[\log q(Wx)\right] + const.$$

$$E\left[\log q\left(Wx\right)\right] + const. \to E\left[\log q\left(y\right)\right] + const.$$

Here, we have further simplified the log-likelihood expression by replacing Wx with our source approximation vector y.

Recall that we define an expectation of a random variable u distributed according to f(u) as

$$E[u] = \int_{-\infty}^{\infty} u f(u) du \tag{2.8}$$

There is a subtle step that needs to be briefly explained by rewriting the expectation term of the log-likelihood in integral form. Recall that q(•) is a hypothesized distribution/density function for our source vector s, based on application specific knowledge. Furthermore, we have y, the approximation of our signal that is a transformed version of s (i.e. y = Zs where Z is a product of W and A) with its own distribution r(•), which changes with W since A is not accessible. The resultant distribution r(•) also happens to determine the nature of the expectation term in our log-likelihood expression. Hence we get

$$\int_{-\infty}^{\infty} r(y) \log q(y) dy + const. \tag{2.9}$$

Which can be rewritten so that the log-likelihood expression can be expressed in terms of the Kullback-Leibler (KL) divergence K[•] and Shannon entropy H[•]:

$$\int_{-\infty}^{\infty} r(y) \log q(y) dy + const. = \int_{-\infty}^{\infty} r(y) \log q(y) \frac{r(y)}{r(y)} dy + const.$$

$$\int_{-\infty}^{\infty} r(y) \log q(y) dy + const. = -\int_{-\infty}^{\infty} r(y) \log \frac{r(y)}{q(y)} dy + \int_{-\infty}^{\infty} r(y) \log r(y) dy + const.$$

$$\int_{-\infty}^{\infty} r(y) \log q(y) dy + const. = -K[r \mid q] - H[r] + const. \tag{2.10}$$

The KL divergence is a non-symmetric non-negative measure of the divergence between the distributions of two random variables. By non-symmetric we mean that

K[r|q] is not necessarily the same as K[q|r]. The KL divergence is a statistical way of quantifying the closeness of two distributions. In the present context, the derived log-likelihood expression incorporates this explicit measure of divergence between the distribution of y = Wx and the hypothesized distribution of the sources (Cardoso, 1998). Maximizing the log-likelihood then becomes a question of finding a W that minimizes the discrepancy between r(•) and q(•) as expressed by the KL divergence.

2.3.3 Information Theoretic Interpretations

Note that the KL divergence term embodies two measures of "mismatch" between y and s. Cardoso (1998) points out a classic property of the KL divergence:

$$K[r \mid q] = K[r \mid r^*] + K[r^* \mid q] \tag{2.11}$$

The term r*(•) represents a product of the distributions such that $r^* = (r^*_1)(r^*_2)...(r^*_n)$. Each r^*_i is equal to the distribution of the corresponding y_i. Note that r*(•) is essentially r(•) without the cross terms. The second KL divergence term is indicative of how far the marginal distributions of the outputs $y_1,...,y_n$ are from the hypothesized distribution. The first KL divergence term quantifies how far apart the output distribution is from the closest distribution with independent entries. Another name for such a measure is mutual information. The mathematical definition for mutual information can be derived directly from the KL divergence-based expression and summarizes the integrals in terms of differential entropy:

$$I(y_1, y_2, ..., y_n) = \sum_{i=1}^{n} H(y_i) - H(y) \tag{2.12}$$

Mutual information is a natural measure of the independence of a given set of random variables (Hyvarinen, 2000). It is always non-negative if and only if the individual entries are independent from one another. The idea of maximizing independence by minimizing mutual information is significant in that it allows us to mathematically justify the idea of achieving maximum independence by maximizing the non-Gaussianity of each component (mentioned briefly in section 2.1). We start by rewriting mutual information in terms of negentropy, which is proven to be a measure of non-Gaussianity (Cover and Thomas, 1991). Negentropy can be thought of as a normalized version of differential entropy in the sense that it is always non-negative. Specifically, it is defined as the difference between the entropy of a Gaussian variable with a similar covariance matrix:

$$J(y) = H(y_{gauss}) - H(y) \tag{2.13}$$

Here, y_{gauss} is a Gaussian random vector whose covariance matrix is the same as y. We can rewrite the definition of mutual information using negentropy instead of differential entropy, constraining the observation vectors to be uncorrelated. The "uncorrelatedness" constraint allows us to avoid dealing with cross correlation terms. The end result is

$$I(y_1, y_2, ..., y_n) = J(y) - \sum_{i}^{n} J(y_i) \tag{2.14}$$

To evaluate Equation 2.14, a timely way of computing negentropy is necessary. Kurtosis-based methods of approximating negentropy suffer from the problems associated with accurately calculating kurtosis (a calculation that is sensitive to the presence of outliers).

An alternate approximation developed by Hyvarinen et al. (Hyvarinen et al., 2000) is

$$J(y_i) \approx \sum_{j}^{p} k_j \left[E\{G_j(y_i)\} - E\{G_j(\upsilon)\}\right]^2 \quad \textbf{(2.15)}$$

Hyvarinen (2000) specifies $G_j(\ )$ to be some non-quadratic equations and k_j some positive constants. The random variable υ is a Gaussian variable of zero mean and unit variance. Hyvarinen (2000) draws attention to the simplest case ($p=1$) so that we have

$$J(y_i) \approx k\left[E\{G(y_i)\} - E\{G(\upsilon)\}\right]^2 \quad \textbf{(2.16)}$$

$$J(y_i) \propto \left[E\{G(y_i)\} - E\{G(\upsilon)\}\right]^2 \quad \textbf{(2.17)}$$

That is, $J(y_i)$ is maximized when the quantity on the right is at maximum. In an optimization framework, we have from Equation 2.17 an objective function for the i^{th} component y_i, dependent on the choice of some G( ).

$$J_G(y_i) \equiv \left[E\{G(y_i)\} - E\{G(\upsilon)\}\right]^2 \quad \textbf{(2.18)}$$

Noting that

$$y_i = w_i^T x$$

where x is the observation vector (which is not variable) and w_i is the i^{th} row of the demixing matrix W (which is variable), we can re-write the objective function as a function of w_i alone:

$$J_G(w_i) = \left[E\{G(w_i^T x)\} - E\{G(\upsilon)\}\right]^2 \quad \textbf{(2.19)}$$

It is possible to optimize our objective function using stochastic gradient descent. Although this can and is done using neural algorithms that allow for fast adaptation to non-stationary signals (Hyvarinen, 2000), the methodology outlined in

Section 2.3.2 involves computations made in batch mode, favouring appealing convergence properties over real-time adaptation (Hyvarinen, 2000).

2.3.4 ICA Implementation Using Newton's Method

In order to find the maxima of $J_G(w)$ (for any individual component) as defined in Equation 2.19, we clearly need to find the maxima of $E\{G(w^Tx)\}$ for certain values of w. Hyavarinen (2000) sums up his development of a Newton's method-based algorithm (built on the assumption of white or whitened data) to find these optima in 4 steps (Hyvarinen, 2000):

1) According to the Kuhn-Tucker condition (Luenberger, 1969), the optima of $E\{G(w^Tx)\}$ under the constraint $E\{(w^Tx)^2\} = ||w||^2 = 1$ are obtained at points where

$$F(w) = E\{xG(w^Tx)\} - \beta w = 0 \tag{2.20}$$

β is a constant based on the optimal value of w. For the purposes of a practical implementation, we use the current value instead.

2) Solving for F(w) = 0 using Newton's method takes the initial form

$$w^+ = w - \frac{F(w)}{\nabla F(w)} \tag{2.21}$$

$$w^* = \frac{w^+}{\|w^+\|} \rightarrow new\,normalized\,value\,of\,the\,current\,vector\,w$$

3) Formally, the Jacobian of F(w), denoted ∇F(w) is defined as

$$\nabla F(w) = E\{xx^TG'(w^Tx)\} - \beta I \tag{2.22}$$

In order to simplify the inversion, we exploit the fact that whitened data allows for the reasonable approximation

$$E\{xx^T G'(w^T x)\} \approx E\{xx^T\} E\{G'(w^T x)\} = I \cdot E\{G'(w^T x)\}$$

This gives us a diagonal matrix whose inverse is straightforward.

4) The final step involves substituting the equation from step 3 and multiplying both sides by

$$\beta - E\{xx^T G'(w^T x)\}$$

This gives us the final form of Hyavarinen's iterative scheme to achieve a single independent component:

$$w^+ = E\{xG(w^T x)\} - E\{G'(w^T x)\} w \qquad \textbf{(2.23)}$$

$$w^* = \frac{w^+}{\|w^+\|} \rightarrow \textit{new normalized value of the current vector } w$$

Hyvarinen further stabilizes his algorithm by adding a step-size parameter μ to the F(w)/∇F(w) term in the second step. When convergence is achieved for a single component, the data set is projected onto the orthogonal complement of this component and the process is resumed. Hyavarinen (2000) refers to this method as a "deflation" scheme.

2.4 APPLICATION OF NLNR AND BSS TO FECG ISOLATION

2.4.1 NLNR Applied to Fetal Electrocardiography

The application of NLNR techniques to abdominal FECG recordings is the focus of research by Thomas Schreiber, Marcus Richter, and Daniel T. Kaplan summarized in papers that were published between 1995 and 1998 (e.g. Schreiber and Kaplan, 1995-

1996 and Richter et al., 1998). Their work extended the idea of reducing noise in deterministically chaotic data to cleaning up noisy electrocardiograms. Eventually this lead them to formulate a method to isolate the FECG from a single abdominal electrode recording by varying the parameters that define the embedding window length (i.e. m and τ) used in the NLNR scheme outlined in section 2.2. More specifically, NLNR is performed twice on the same mixed MECG/FECG signal. It is first performed such that the fetal component is removed along with regular noise. Subtracting the resulting signal containing only a maternal component from the original gives an approximation of a fetal signal plus noise. The procedure is then repeated on the original data with a shorter embedding window and a smaller neighbourhood size in order to obtain a relatively noise-free MECG/FECG signal. The fetal component is estimated as the difference between the two resulting signals as illustrated in Figure 2.3. The methods proposed by Richter et al (1998) is slightly modified to account for the case when the noise amplitude is comparable to the peak-to-peak amplitude of the FECG, making the separation of the MECG/FECG and the noise more difficult. Thus, NLNR with slightly altered parameters is performed directly on the fetal-noise signal rather than subtracting from it a signal containing only noise.

Further, the specific parameters (m, τ, and the nearest-neighbour dimension p) that give the best results with respect to a particular effect were found through experimentation (Richter et al., 1998) and are summarized in Table 2.1.

m	τ (in ms)	p	Comment	Result of using NLNR with these m, τ, and p values
10	4	10	The delay vector length is 40 ms (average maternal R-R interval is 800 ms – roughly twice that of fetus)	Performed on the original signal. The result is an MECG only signal which is subtracted from the original signal, yielding FECG+noise
10	2	3	Smaller neighbourhood size and embedding window length means finer resolution in delay space	Performed on the FECG+noise signal. The result is a reduction in the noise but not an elimination of the FECG component

Table 2.1 Parameter values for NLNR used in the FECG separation process in (Richter et al., 1998).

One of the main advantages of this process is that the data acquisition process is simplified by the fact that only one signal is necessary. However, baseline fluctuations in the signal can cause problems by causing the clusters of delay vector co-ordinates to be less cohesive.

2.4.2 BSS Applied to Fetal Electrocardiography

The application BSS techniques to abdominal FECG recordings is the focus of work done by Lieven De Lathauwer and his colleagues at K. U. Leuven in Belgium and is mentioned in articles by De Lathauwer et al. (2000) and Zarzoso and Nandi (2001). In some ways ICA goes further than any other techniques in isolating the fetal signal because it is not only trying to enhance and/or attenuate certain parts of abdominal signals, but actually attempting to identify and invert the mixing process that makes FECG extraction problematic in the first place. In addition, the distribution of ECG signals is favourable in an ICA context since they are clearly non-Gaussian (Figure 2.4).

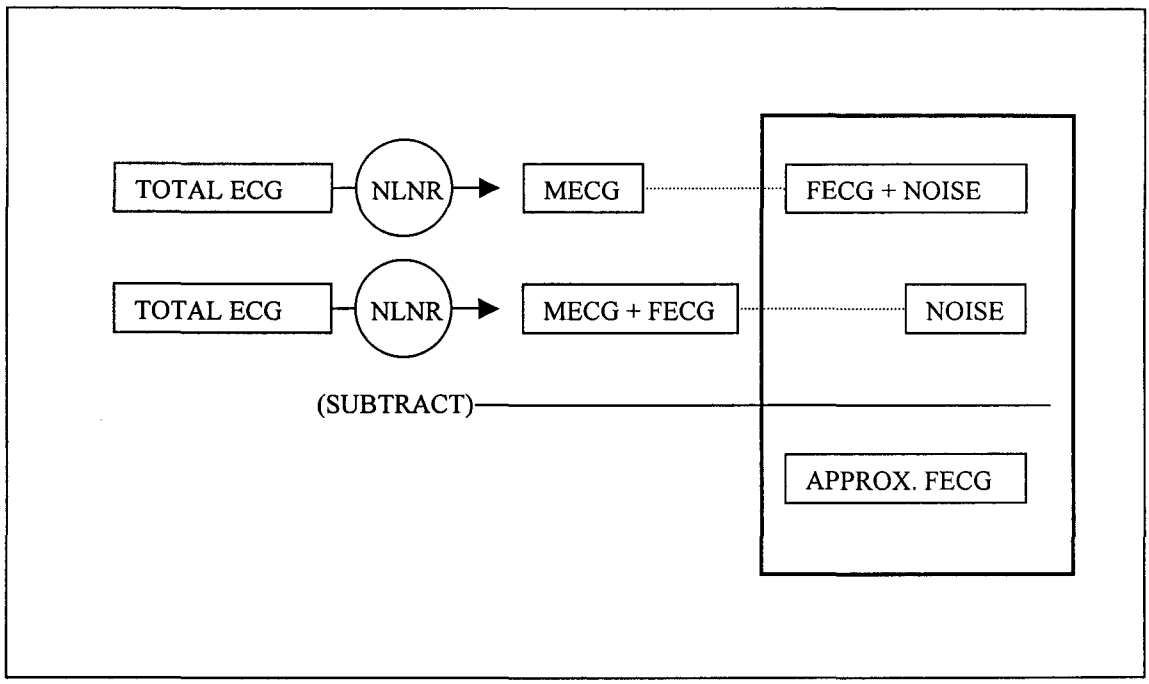

Figure 2.3 Schematic diagram for the extraction of the fetal ECG. Two locally linear projections are performed. The fetal component is estimated as the difference of the two resulting signals. Sometimes, it can be useful to perform an additional noise reduction step on the estimated fetal ECG signal, with an additionally lower neighbourhood diameter and delay vector length (Source: Schreiber and Kaplan, 1996).

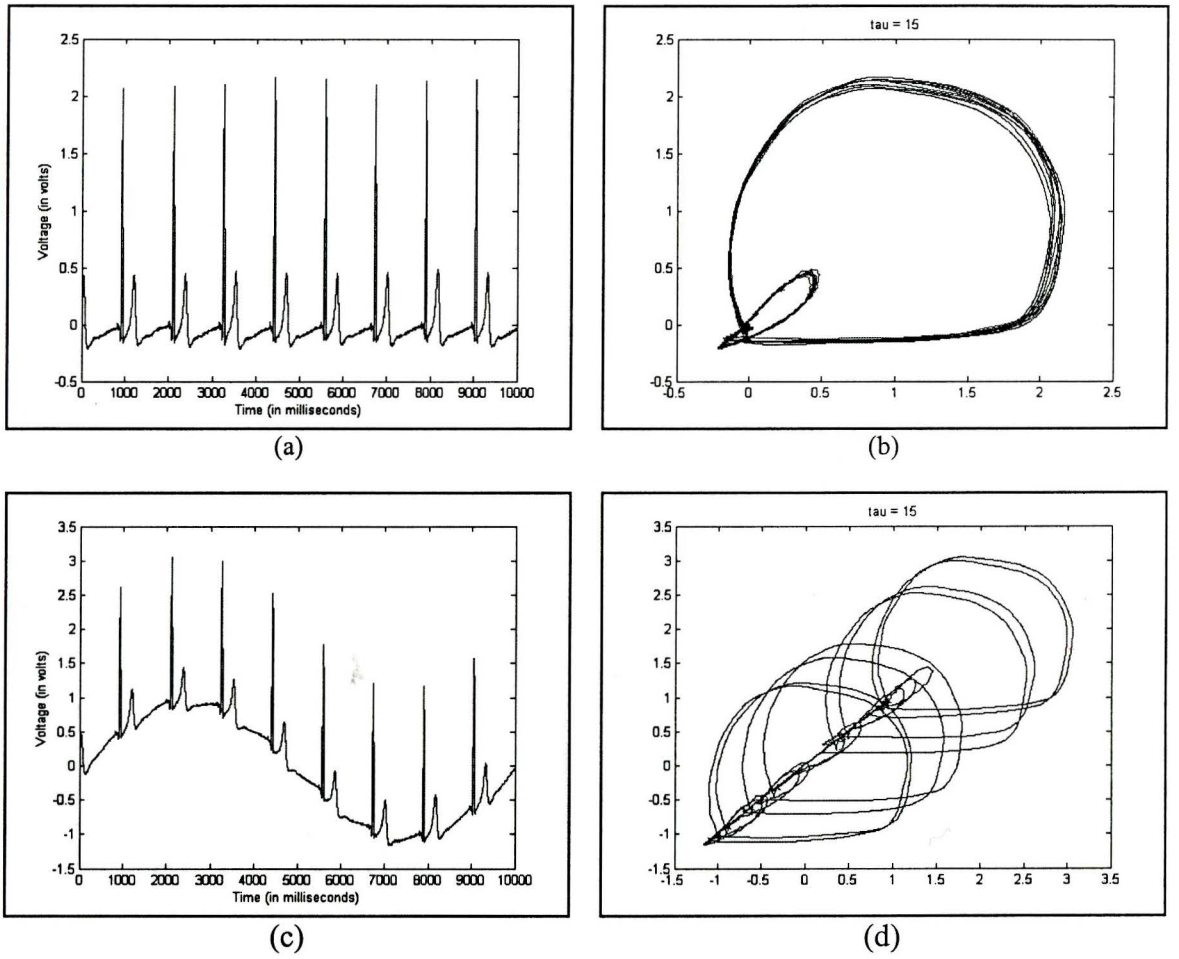

Figure 2.3 Demonstration of the effects of low frequency noise (e.g. muscle movement) on an ECG's delay space representation. The ECG sample in (a) has been combined with a sinusoidal signal resulting in the signal shown in (c). The associated delay space representation in (d) shows how the manifold is increasingly ambiguous.

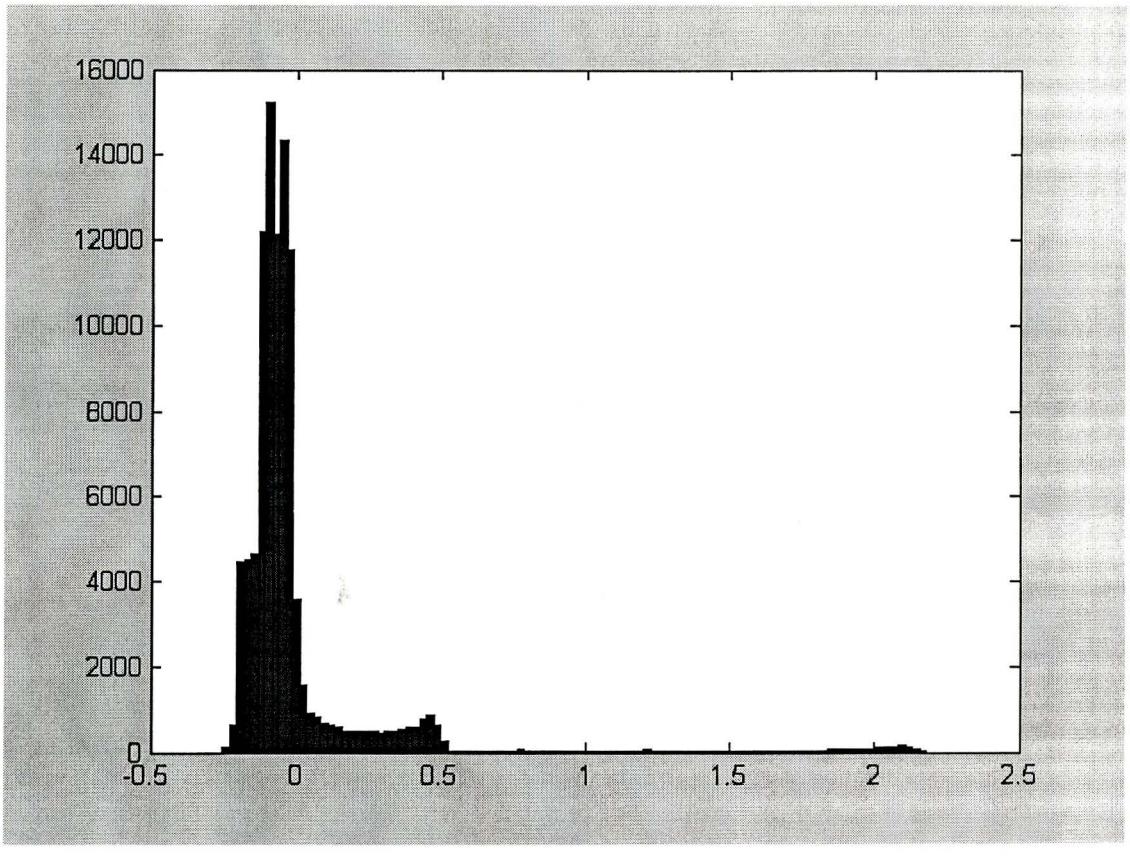

Figure 2.4 Demonstration of the non-Gaussianity of ECG signals. The histogram of a typical ECG signal has a highly skewed distribution. In particular, the R-wave results in a long right-hand tail.

2.4 SUMMARY

The nonlinear noise reduction technique outlined in this chapter works well with quasi-periodic signals in particular because the "clustering" of delay vector co-ordinates in delay space allows for the eigen-analysis to yield plausible linear approximations. However, the noise reduction scheme appears to have an inordinate number of parameters that need to be optimized, and it is not clear as to what the quantitative objective of this optimization should be. One goal of this thesis is to obtain a range of values for which both FECG waveforms and noise components can be separated from a mixed signal.

In contrast to the nonlinear noise reduction technique blind source separation requires less application specific adjustments before the data is actually processed. One can say, moreover, that the non-Gaussian nature of ECG signals makes successful separation likely.

Chapter 3

Recording Apparatus and Protocol

3.1 OVERVIEW

The objective is to design and build a data acquisition system that can amplify and digitize the electrical activity within the abdomen of a pregnant woman. This chapter describes the main components of our system including:

1. Transducers to convert the electrical activity recorded from the surface of the body
2. High quality amplifiers with attractive SNR properties
3. A subsystem to digitize and record the signals for further processing offline (possibly on a different computer system).

Although the design is not constrained to be portable, the preference is for the overall setup to be non-intrusive. In addition, this chapter outlines a detailed procedure for recording signals from the maternal abdomen.

3.2 APPARATUS

3.2.1 Electrodes

Standard ECG conductive adhesive electrodes are cheap, widely available, do not require additional electrolyte jelly and are designed to fit a widely available ECG leads with button clips. However, given that the initial stages of the recording session requires the technician to find the optimal electrode location through some type of exploratory process, the adhesive electrodes prove to be less than ideal since they are designed for single use and constant sticking and unsticking of such an electrode would be unpleasant for the patient. An alternative to adhesive electrodes is to use bulb electrodes that consist of a small metal cup with a hole in that leads to a rubber bulb. Used in conjunction with an electroconductive jelly, these electrodes allow the technician to continuously adjust the position of the electrode and secure its various temporary positions by using the suction generated by deflating the bulb. Since prolonged use of bulb electrodes in one spot causes reddening of the skin due to the suction, it is probably best to substitute them for adhesive electrodes once a suitable electrode location is found. The impedances for the bulb electrodes and leads were all measured to be between 1.3 and 1.5 Ohms each.

3.2.2 Amplifiers

In light of the inherently weak fetal signal (which can sometimes be comparable to noise levels), there is a priority on having high-quality amplifiers available for recording. Due to the availability of off-the-shelf ECG monitors and the low priority for portability, amplifier circuitry was not custom built at this time. The Spacelabs 90721 neonatal monitors used for recording purposes have the following amplification specifications:

Gain	1000
Bandwidth	0.2 Hz to 40 Hz at 3 dB points
CMRR	100 dB at 60 Hz
Filtering	Line Frequency (50 Hz/60 Hz) notch filter

Table 3.1 Spacelabs 90721 neonatal monitor amplifier specifications

For the short to midterm, the Spacelabs 90700 series ECG monitors are fully supported by local offices and warehouses, and the acquisition of parts and documentation does not appear to be problematic. They are a viable alternative to smaller custom-built ECG amplifiers while such devices remain under construction.

3.2.3 Digitization

Analog-to-digital conversion is accomplished by a DataQ CODAS System installed on a 486-powered personal computer. The specifications for the onboard analog-to-digital converter are outlined in Table 3.2.

Resolution	12-bits
Total Input Channels	16
Range	-2.5 V to 2.5 V
Overall Throughput	50 kHz

Table 3. 2 DataQ CODAS system digital-to-analog conversion board specifications

Aside from the general bulk of computer and the relative lack of onboard computing power for immediate analysis, the CODAS data acquisition unit is more than adequate for the collection of data, especially considering the high throughput of the converter. A preferred solution is a Pentium-based laptop computer running the increasingly popular LabView data acquisition/analysis suite from National Instrument.

3.2.4 Assembled Apparatus

The overall hardware setup fits on a cart with the monitors occupying the lower shelf and the data acquisition hardware occupies the top. The metallic cart includes a 10-gauge grounding wire, which connects the cart to the patient bed for optimal grounding (the monitors are designed to be grounded to their respective casings which are in contact with the cart). All electronic components are plugged into a hospital-grade power bar and the entire unit is then isolated by and isolating transformer. A diagram of the recording suite is pictured in Figure 3.1.

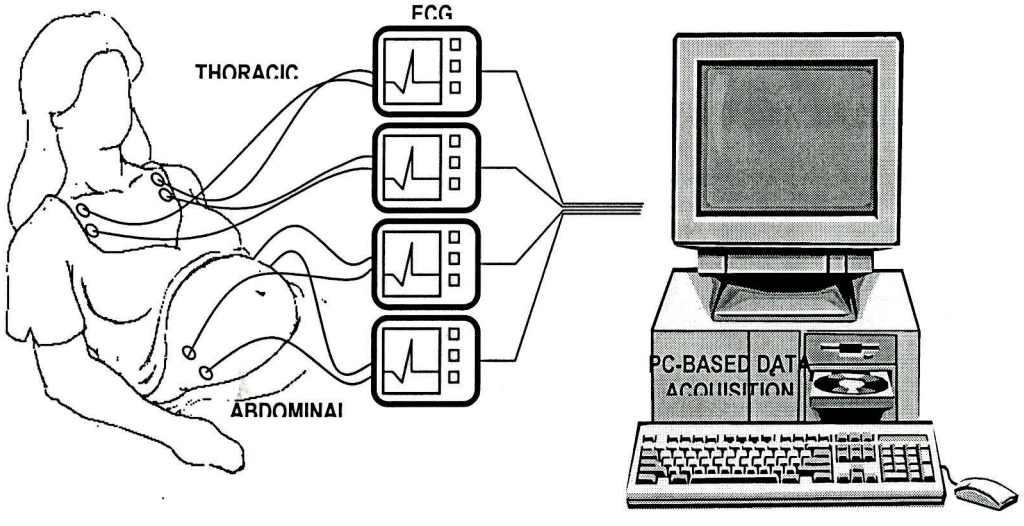

Figure 3.1 Diagram of apparatus used for abdominal recording.

3.3 RECORDING PROCEDURE

One of the constant challenges of employing abdominal ECG's for any type of diagnosis has been the difficulty in obtaining a useful fetal signal. Optimal recording of the fetal signal is a combination of (a) medical expertise, (b) obtaining the maximum amount of prior information about the fetal position, and (c) an exploratory electrode placement process that takes advantage of the previous two factors. In many of the articles that focus on using abdominal recordings for fetal diagnoses there is much written about the nature of the FECG signal with respect to anatomy and physiology. However, there is very little written of a systematic method to actually record the data and this is where assistance from physicians and nurses experienced in performing abdominal recordings becomes crucial. The protocol presented in section 3.2.3 reflects a combination of information from obstetrics texts, experience from previous experiments, and knowledge obtained through the course of the initial stages of the current recording sessions.

3.3.1 The Nature of FECG Recording

The pumping action of a human heart is the result of the nervous system initiating an electrical wavefront, which propagates across the heart. The subsequent electrical current causes potential differences to exist on different point of the body. These potentials are what ECG equipment is designed to detect and record. The now well-known ECG waveform has direct interpretive value concerning the mechanical function and the health of different heart muscles. The FECG is no less relevant for investigating the health of the fetus. However, recording the fetal ECG before term is made

challenging by several factors. Potential measurements made on the mother's abdomen contain contributions from several bioelectric phenomena (e.g. maternal, and fetal heart activity, potential distributions generated by respiration and stomach activity, uterine muscle contractions). In addition, there are several sources of noise (e.g. 60 Hz line noise, thermal noise, electrode impedance). Lastly, difficulties in recording the FECG using abdominal electrodes arise from factors inherent to pregnancy such as the impedance brought on by the development of the vernix caseosa and the placenta at different stages of pregnancy, and the patient-to-patient variability in obesity, fetal position, and fetal geometry. Each of these aspects of recording the FECG from abdominal electrodes needs to be addressed in the recording protocol.

3.3.2 Recording Protocol

The protocol outlined in this section is derived from a combination of direct medical expertise, experience, and insights into abdominal recording featured in (Freeman, 1991). Volunteers were chosen and approached by Dr. Barbara Brennan of McMaster University Medical Center (MUMC) and consent is obtained formally through a written form that is witnessed and signed. Dr. Patrick Mohide of MUMC observed that the optimal stage in pregnancy for abdominal recording is between 24 and 26 weeks. Prior to this window, the fetal signal is too weak and afterwards the impedance from the tissue and fluid surrounding the fetus becomes too great. When available, the attending physician first determined fetal position and the approximate location of the fetal heart. This procedure requires the use of ultrasound equipment and takes anywhere from 15 to 20 minutes.

Once a reference point was decided upon, a line from that point to the maternal heart was noted and used as the cardiographic midline. Optimal electrode placement was then found through an exploratory ECG process. One monitor was activated and the ground lead for this monitor was attached to the patient's leg via a plate electrode or a simple adhesive electrode. Next, the first suction electrode was placed in the supra-pubic region as close to the midline as possible. This particular region has been found to have the least amount of signal impeding tissue. Staying on the midline and relative to the first electrode, the second suction electrode was placed an equal distance on the opposite side of the approximate fetal heart position. This second position may correspond to an infra-umbilic position. While watching for improvements in the FECG waveform amplitude, the second electrode was moved from side to side. Here, Freeman (1991) advises moving the electrode away from the fetal small parts and the possibility of tilting the mother's position for improving the fetal signal. Locating an optimal electrode location often required an additional 20 minutes.

For recording purposes the suction electrodes were substituted with adhesive electrodes. For four abdominal channels, four pairs of electrodes were placed in a cluster around the optimal electrode location. The remaining monitor was used for the maternal thoracic (chest) ECG recording. During a five-minute recording, the subject was asked to remain as still and relaxed as possible to minimize motion and respiratory artifacts.

3.4 SEPARATION SOFTWARE

The algorithms outlined in Chapter 2 are both implemented as Matlab functions and scripts. Specifically, the NLNR Matlab code was written by the author according to the methodology outlined by Schreiber and Kaplan (1996) and the ICA Matlab code is the FastICA package written by Hugo Gävert based on Hyavarinen's fixed point ICA algorithm and is available from Helsinki University's website http://www.cis.hut.fi/projects/ica/fastica/.

In addition to the Matlab implementations, both techniques have been re-written in C-code making the analysis tools more widely available to the collaborating physicians as well as reducing the computation time. All code written by the author over the course of this thesis is available upon request.

3.5 SUMMARY

It is very likely that the overall recording procedure will evolve with the number of recordings that are made. We have assumed that amplifiers with CMRR of 100 dB is sufficient to ensure that the fetal signal can be recorded using skin electrodes attached to the abdomen. We have also assumed that the neonatal amplifier gain is sufficient to yield recognizable FECG. The validity of both assumptions requires the analysis of the recorded data and continuous consultation/discussions with medical experts.

Chapter 4

Results and Analysis

4.1 OVERVIEW

The NLNR technique was tested using synthesized mixed ECG primarily to ascertain the effects of changes in the various parameters. The results from these tests offer insight into ways of efficiently finding effective parameters for real physiological signals such as MECG and FECG. Since the BSS technique is a form of blind identification, it is much more meaningful and timely to apply the BSS algorithms to real-world mixtures rather than synthesizing and simulating a mixing matrix and multiple sources. Several recordings were made over the course of the writing of this thesis. It should be noted that the final recording protocol outlined in Section 3 evolved to its documented form while these recordings were being made.

4.2 ABDOMINAL RECORDINGS

Five abdominal recordings have been attempted to date (Table 4.1). Of these five sessions, only on the last four occasions was any signal recorded. The FECG is not evident in any of these recordings. The recordings served more as opportunities to familiarize the relevant staff with the recording procedure and to bring attention to issues such as the necessity for a systematic scheme to position the electrodes and the necessity to employ suction electrodes for exploration purposes and use adult-sized adhesive electrodes for the actual recording. More importantly, the abdominal recordings are useful in providing a "real" signal environment (minus the fetal signal) for better simulations. Segments of our recordings (Figure 4.1 – Figure 4.4) clearly show the presence of the various artifacts that are inherent to abdominal recordings. Figure 4.5 illustrates how a suitably scaled and subsampled ECG signal is added to simulate the absent FECG component in the recorded signal.

Subjects Initials	Gestation (weeks)	Length of Recordinng (minutes)	Comments
KG	36	-	- A/D converter malfunction → no ECG
SM	27	5	- Inadequate grounding wire results in abundant 60 Hz noise - Neonatal electrodes used (less obtrusive)
DE	32	2	- Better grounding wire - Adult electrodes used (stronger signal)
SM	30	5	- Introduced use of suction electrodes for initial electrode positioning
JW	35	3	- New electrode positioning protocol (ultrasound used to determine approximate fetal heart position) - Reference electrode for abdominal ECG seems best on when placed on back of patient

Table 4.1 Summary of recording sessions made at McMaster University Medical Center.

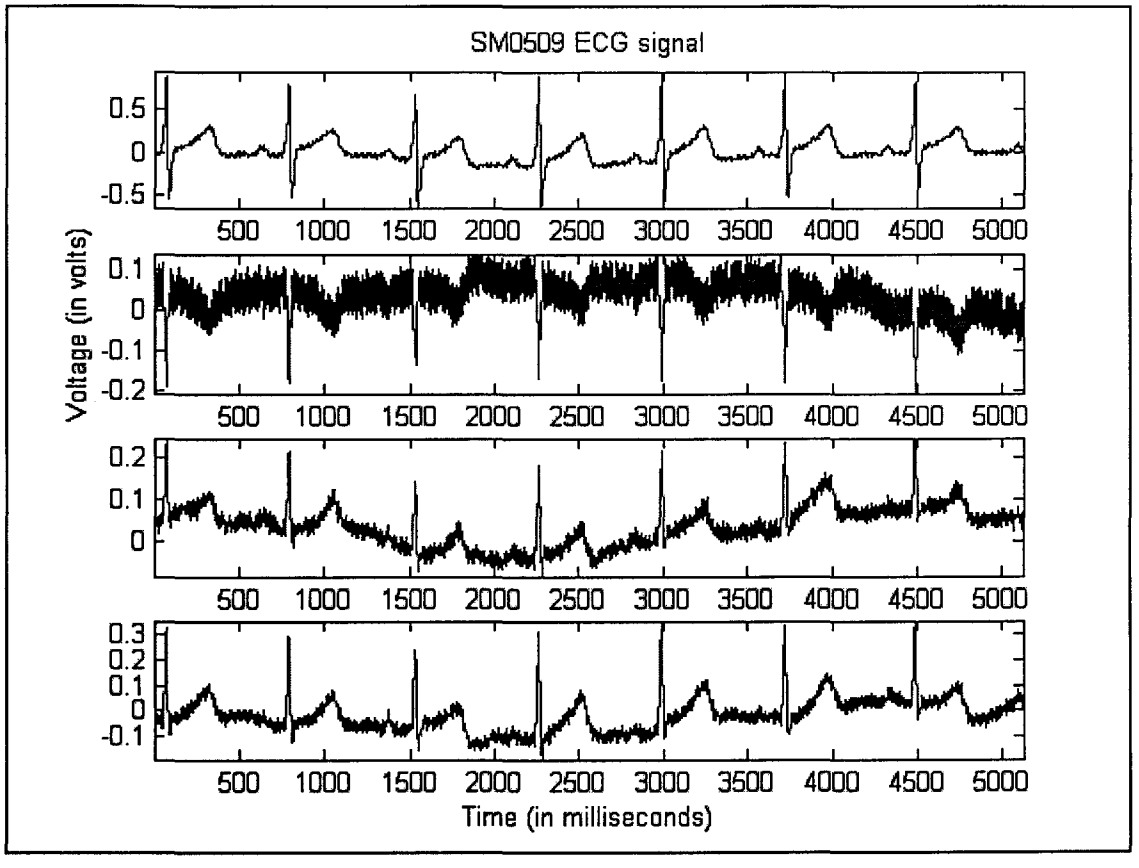

Figure 4.1 Sample of a 4-channel abdominal recording made at McMaster University Medical Centre. Note the increased amount of 60 Hz noise in channel 2 (second row). For this recording, all channels were used for abdominal signals and no thoracic ECG was recorded.

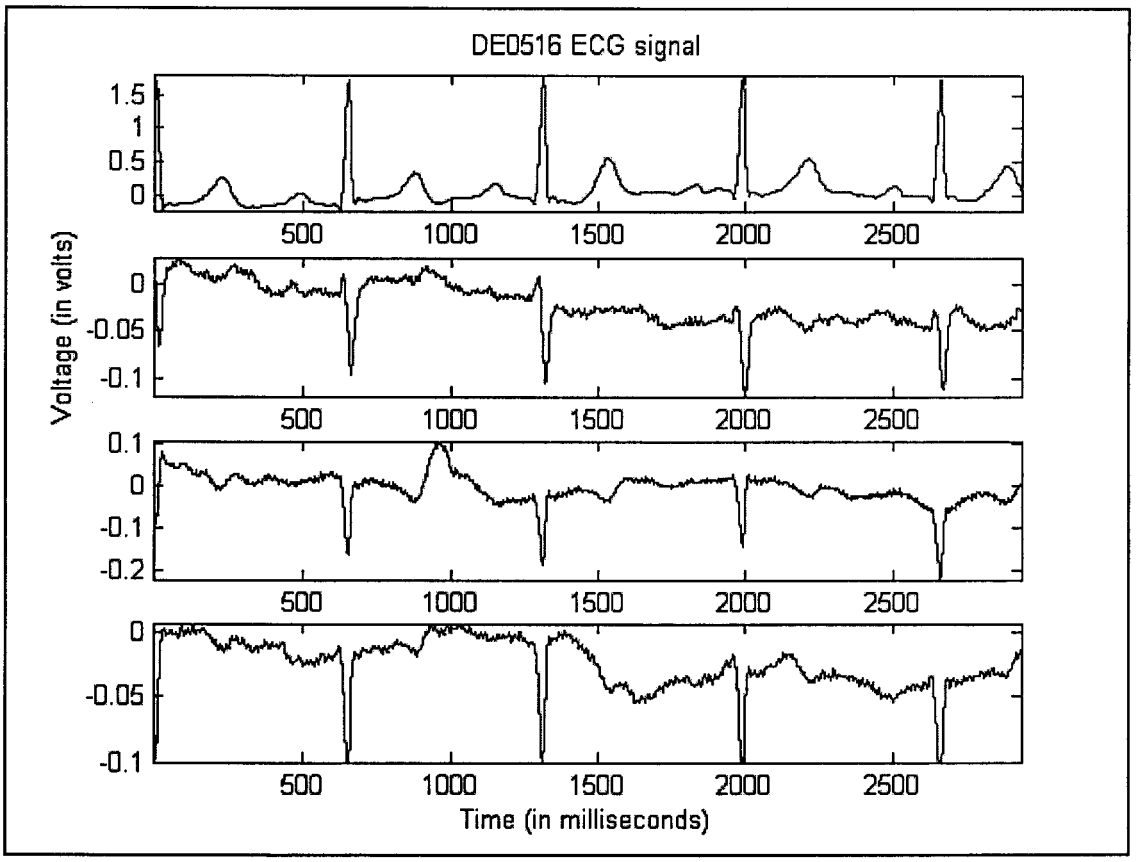

Figure 4.2 Sample of a 4-channel abdominal recording made at McMaster University Medical Centre. Note the inversion of the R-wave in the abdominal channels (channels 2, 3, and 4) and the lower amplitude of MECG components.

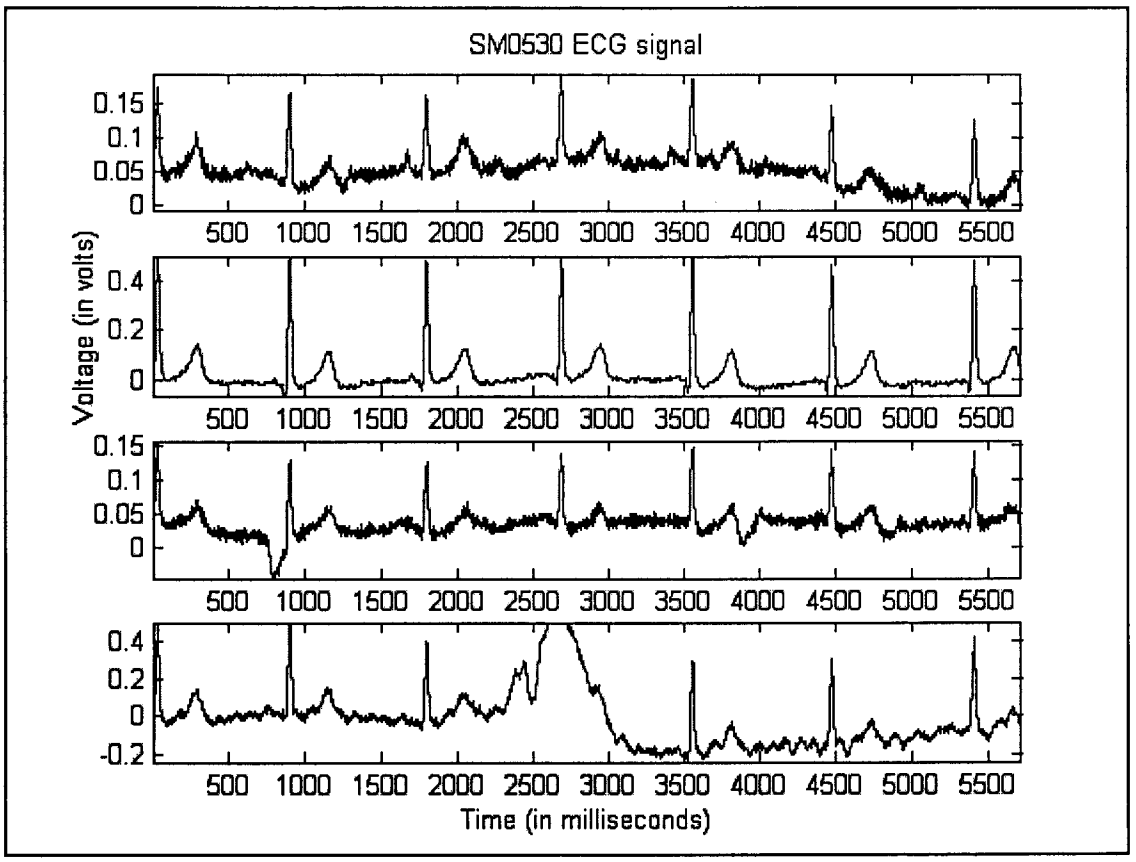

Figure 4.3 Sample of a 4-channel abdominal recording made at McMaster University Medical Centre. Note the motion artifact from fetal movement in the abdominal signal at the bottom. The thoracic signal is second from the top and is weakly amplified.

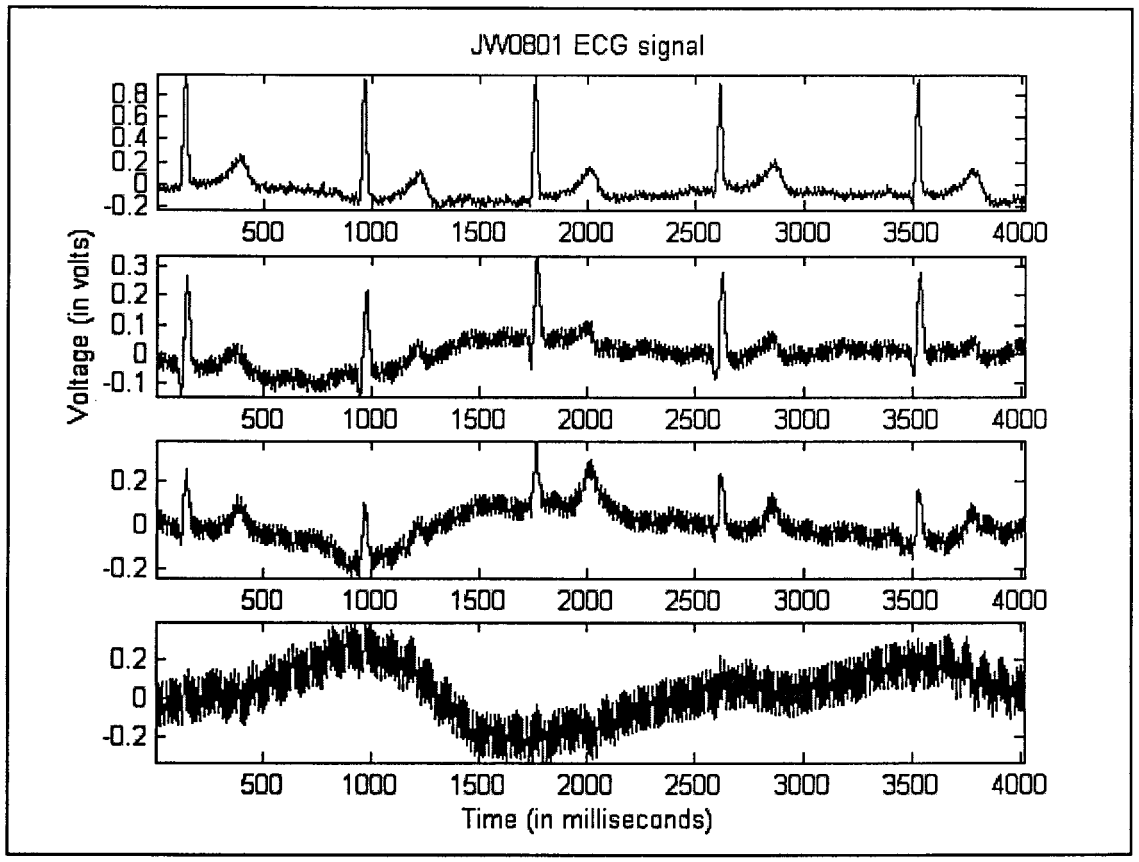

Figure 4.4 Sample of a 4-channel abdominal recording made at McMaster University Medical Centre. 60 Hz appears to be problematic in this recording as well.

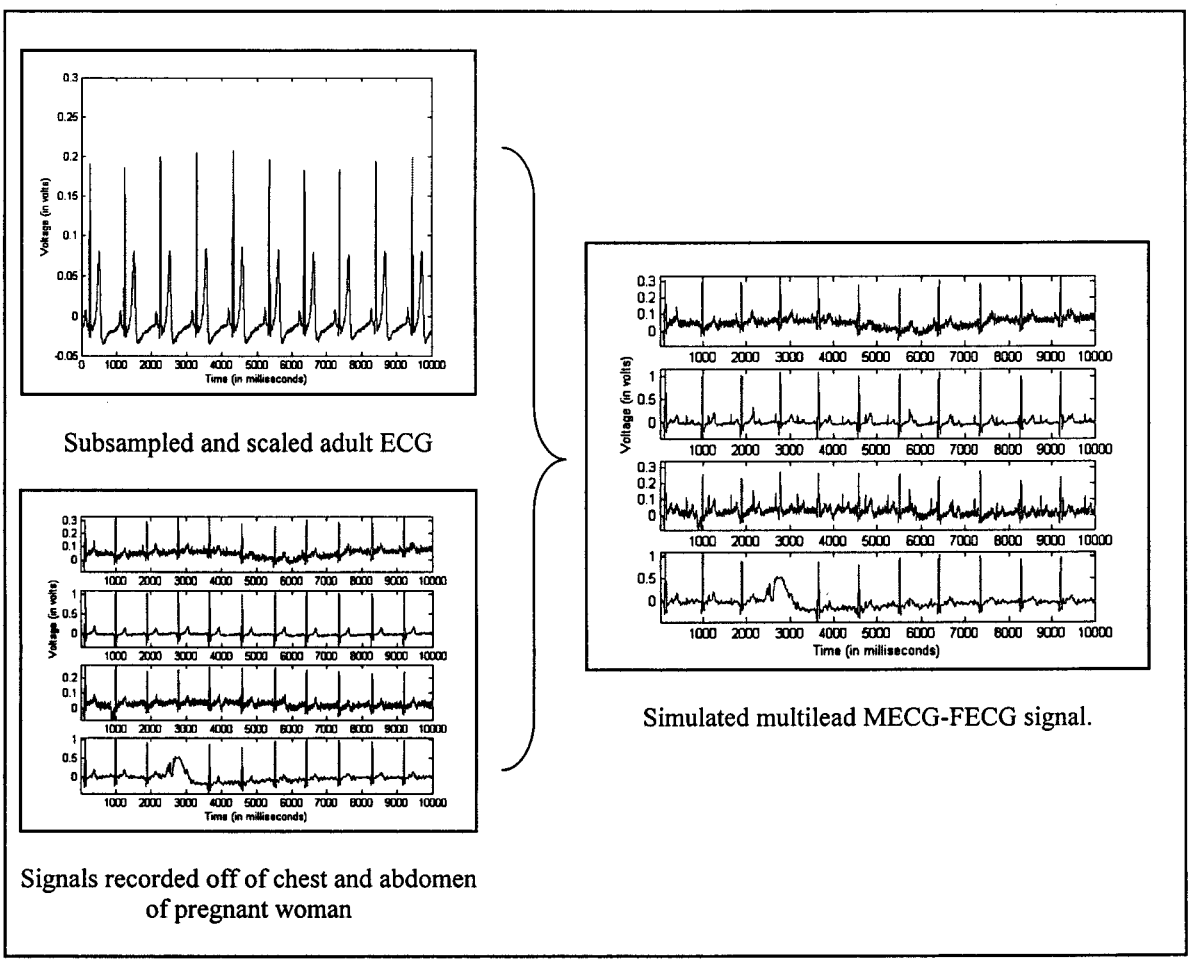

Figure 4.5 Example of combining simulated FECG signal and actual (filterd) abdominal recording. The filtering is meant to reduce the line noise and some of the baseline drifting. Note that the FECG is not added to the first channel, which was recorded from chest leads (lead II ECG).

4.3 NOISE REDUCTION OF A SYNTHETIC MECG-FECG SIGNAL

For initial testing of the NLNR algorithm two adult ECG's sampled at 500 Hz were artificially mixed together to simulate the mixed MECG-FECG signal from the abdomen of a pregnant patient. One of the two signals was subsampled to have an approximate R-R interval of 500 ms (roughly half the size of an adult R-R interval) and scaled to be approximately a fifth of the amplitude of the other ECG. This is based on tracings observed in previous articles (Hon and Lee, 1963; Bemmel, 1968; Crowe et al., 1996) and on a previous occasion at McMaster University Medical Centre. Figure 4.6 illustrates a sample of the mixed signal and its two-dimensional delay space representation. In order to assess the optimal parameter values (since the process of finding these values is not discussed by Schreiber and Kaplan), we perform a bank of tests for parameter adjustments and observe the effects on the FECG component of the simulated mixed signal.

The NLNR is a process that is capable of filtering out different components found in the ECG signal based on duration of signal components (by adjusting the embedding window length defined as $(m-1)\tau$) and the amplitude of signal components (by adjusting the nearest neighbourhood via the neighbourhood radius) (Richter et al., 1998). The aim of these experiments is to find the optimal values for these parameters and develop some intuition about the effects of varying these parameters. We believe this practical expertise will lead to better signal analysis in the future.

4.3.1 Embedding Window Length

The first set of tests involves adjusting the τ parameter while keeping $m = 10$. Recall from Figure 2.1 that the embedding window length value is directly associated with how the manifold "unfolds" in delay space. Figure 4.7 shows the results of varying τ. The fact that the MECG is well-preserved while FECG is attenuated for certain values of τ shows how the NLNR technique differs from traditional frequency based filtering that would filter out parts of both the MECG and FECG.

In particular, the maternal ECG waveform is nearly unaffected by the NLNR process. The fact that the MECG waveform is not affected (especially the R-wave) helps to overcome the difficulty in matching the amplitudes of the maternal components when the processed signal is subtracted from the original mixed signal. This difficulty is exactly what makes simply subtracting a thoracic signal from an abdominal signal problematic. The attenuation of the fetal signal around the T-wave is particularly good largely due to the uniqueness of T-wave related points in delay space. Also, there appears to be a "ringing" phenomenon about the FECG waveforms as τ is greater than 15 (Figure 4.7e and Figure 4.7f). In fact, the attenuation of the FECG in Figure 4.7f is about the same as that in Figure 4.7b except with additional noise. One may recall that increasing the embedding window length (i.e. $(m-1)*\tau$) also resulted in a worse delay space representation (Figure 2.1e). In this case, the embedding window for what is nearly an ideal signal whose FECG is suppressed and whose MECG is conserved appears in Figure 4.7c is 90 samples or 90 ms at a 1000 Hz sampling rate– roughly a tenth the time between successive heart beats for an adult and little less than fifth the time between

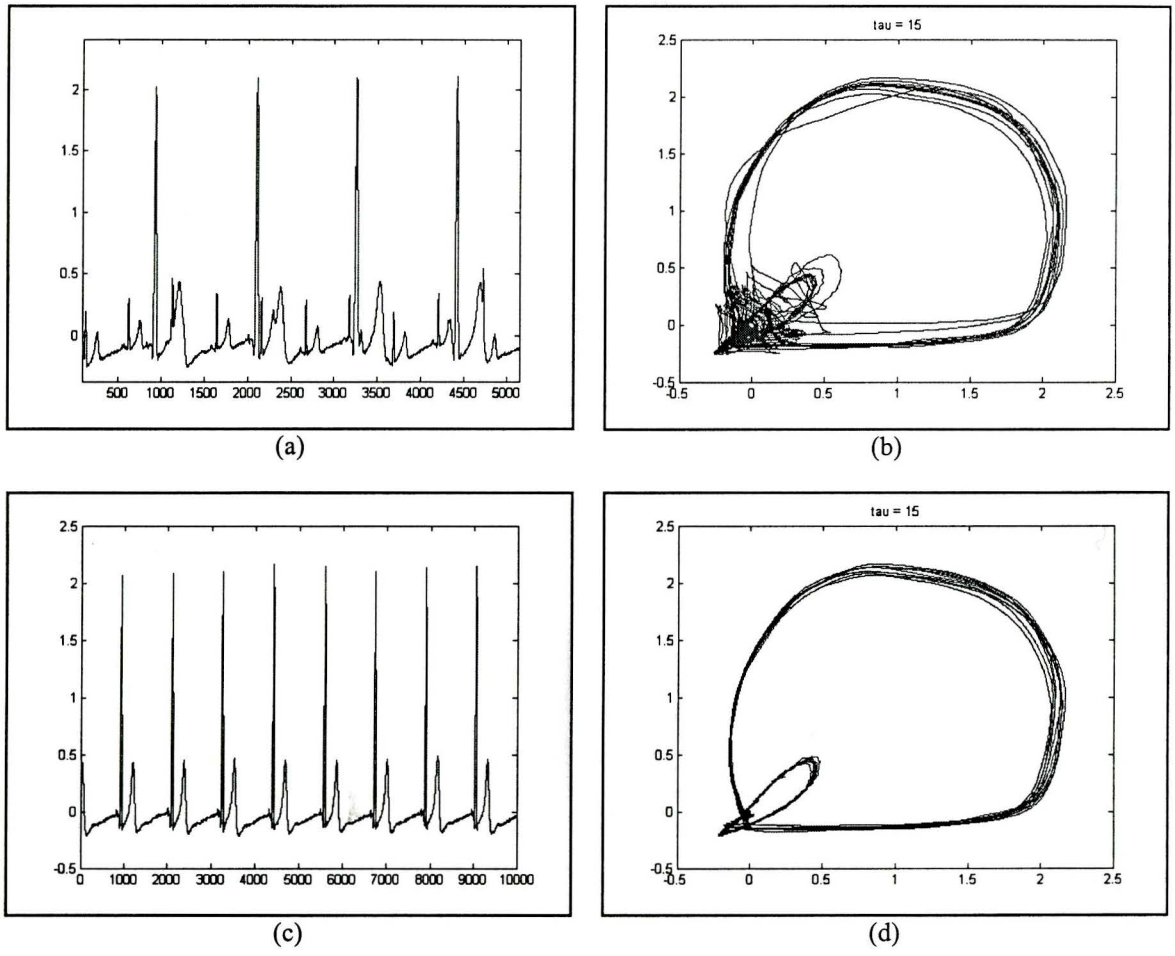

Figure 4.6 Comparing the mixed ECG delay space representation in (b) with the delay space representation of a normal ECG signal in (d). The associated ECG signals (sampling rate 1000 Hz) appear in the left hand column. The effect of the second ECG signal leaves the QRS complex of the "maternal" signal relatively uncorrupted. The idea is to project the "deviated" points back onto the approximate manifold associated with the quasi-periodic ECG.

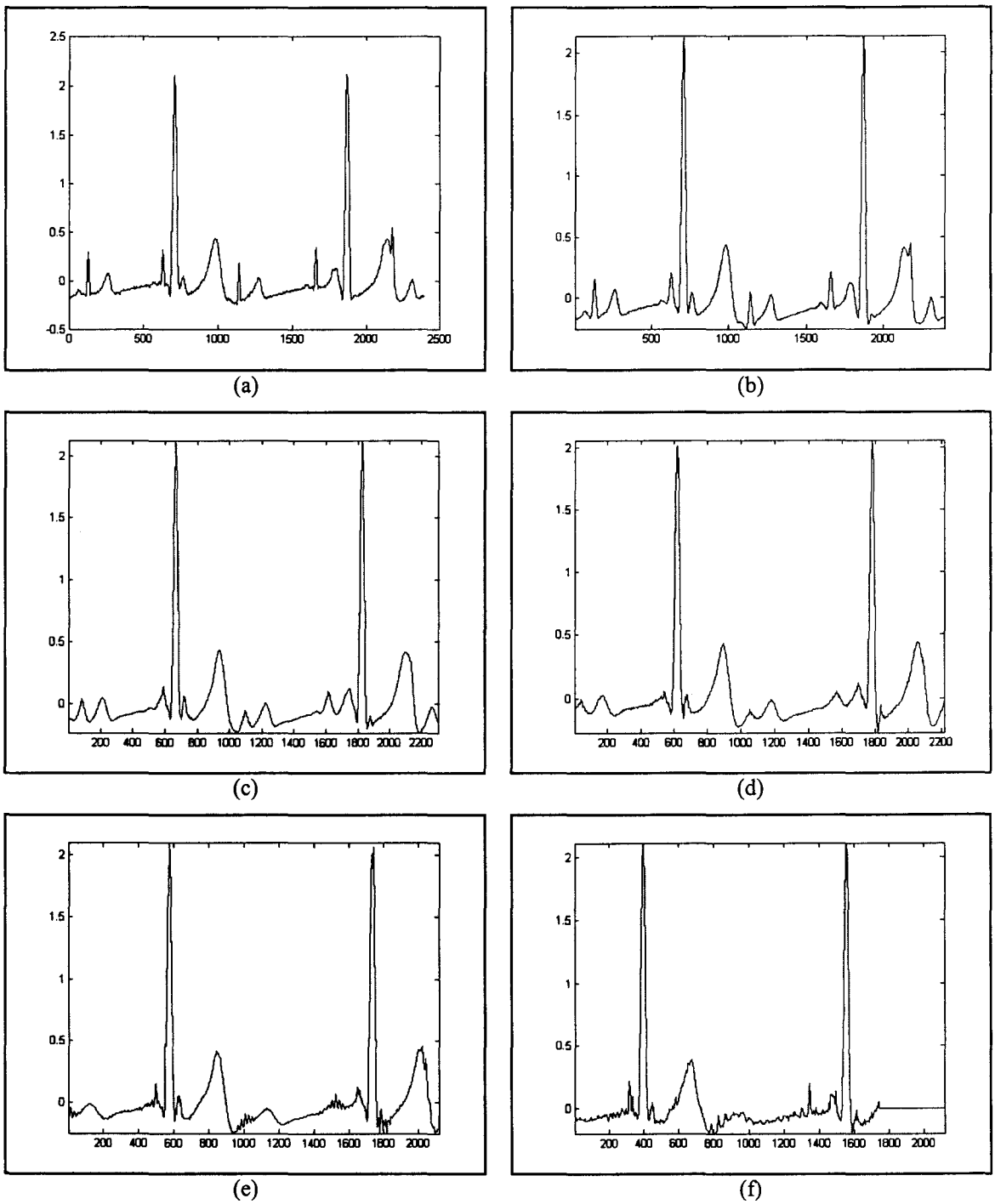

Figure 4.7 The effects of varying the τ parameter. (a) The original mixed signal. The NLNR-processed signals show how the FECG signal is increasingly attenuated while the MECG remains practically unaffected. (b) τ=5 (c) τ=10 (d) τ=15 (e) τ=20 (f) τ=40. The bottom right result is beginning to show signs of "ringing" around the locations of the FECG waveforms.

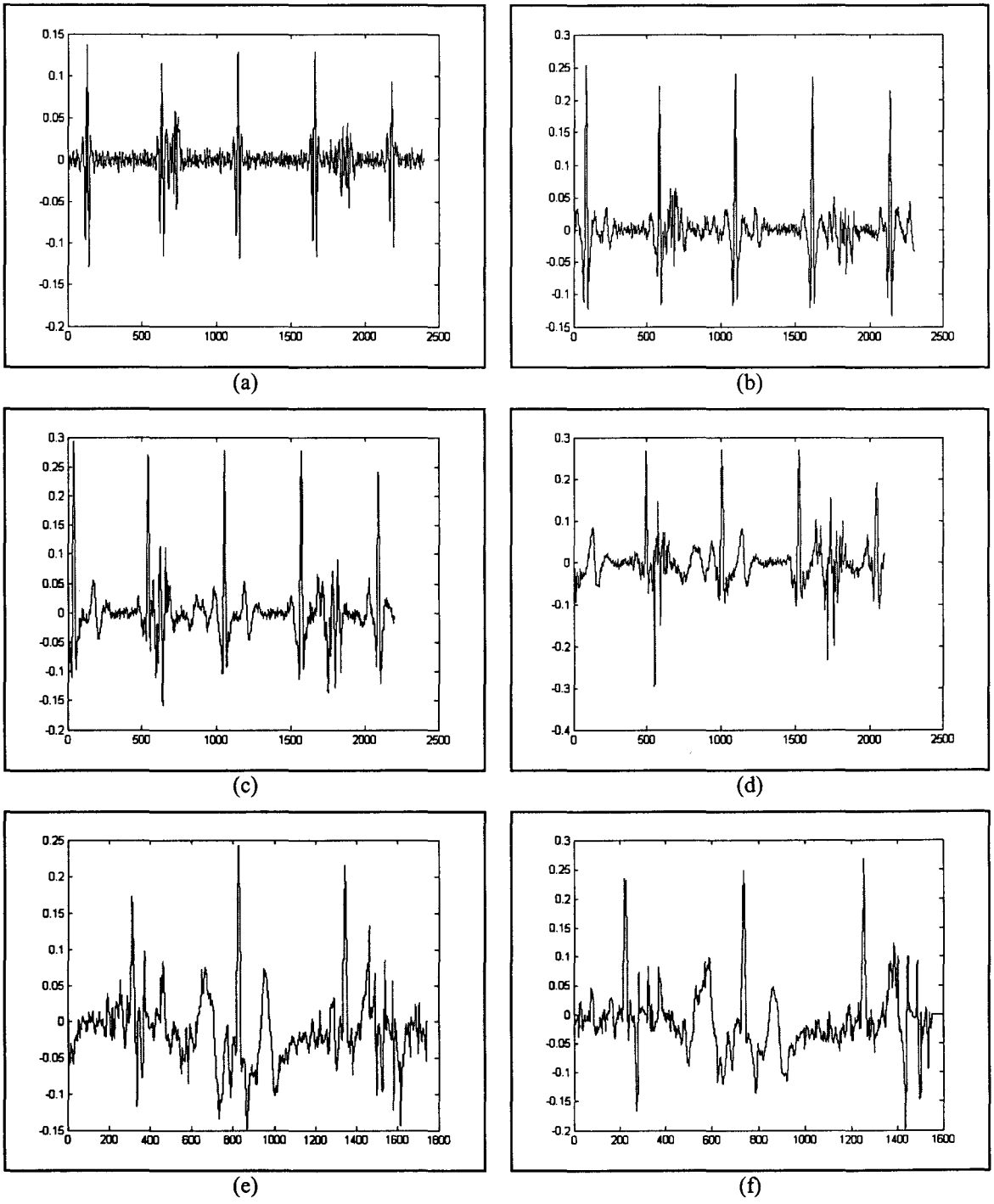

Figure 4.8 Approximate FECG signals from subtracting the processed signal from the original signal for various values of the τ parameter. (a) τ=5 (b) τ=10 (c) τ=15 (d) τ=20 (e) τ=40 (e) τ=50. The optimum value of τ is approximately 5 to 10. The approximate signal becomes increasingly "noisy" due to the fact that an increased embedding window used in the NLNR process creates a greater difference between the desired signal component of the original signal and the processed signal.

successive heart beats for an adult and little less than fifthe the time between successive fetal heart beats. The effectiveness of the NLNT process is more evident in Figure 4.8, which illustrates the result of subtracting the processed signal from the original signal.

Given an embedding window of 90 ms, we tried varying the parameter m only to discover that above $m = 10$, there is very little difference in the resulting approximate FECG signal. This makes sense since m represents the dimension of the subspace occupied by the mixed MECG-FECG signal. Increasing number of dimensions above the dimension of the subspace should have no effect on the separation process.

4.3.2 Nearest Neighbourhood

A series of experiments were run to determine the effects of varying the parameters associated with the nearest neighbourhood search in delay space. This includes the size of the nearest neighbourhood (in terms of the delay space plots, this would be the number of total points) as well as the radius. It should be noted that in the implementation of the NLNR process, the nearest neighbourhood radius exponentially increases from its initial value until a predetermined number of delay coordinates are found. Our tests demonstrate that a small neighbourhood radius (e.g. Figure 4.9a) causes the NLNR process to insufficiently suppress the FECG component. On the other hand, too great a radius causes the MECG to be increasingly suppressed, causing problems in the subtraction process. The ideal size of the radius appears to be lie between the maximum amplitudes of the MECG and FECG signals.

Finally, the total number of delay coordinates used for a "correction" iteration was varied as well. The number of delay coordinates equivalent to 1-2 ECG cycles was

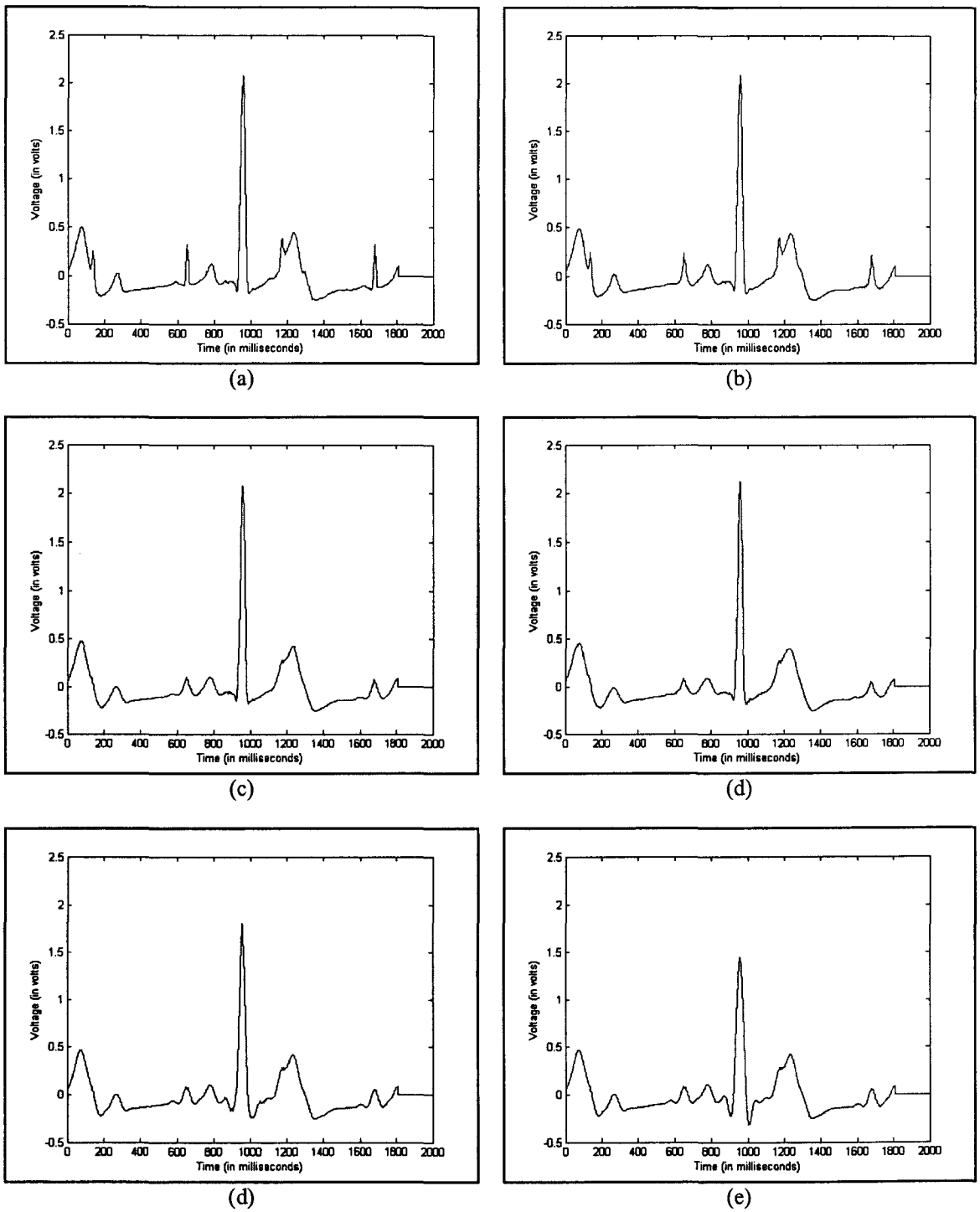

Figure 4.9 The effects of varying the nearest neighbourhood radius. The NLNR-processed signals show how the FECG signal is increasingly attenuated for increased radius length epsilon (a) epsilon=0.5 (b) epsilon=1 (c) epsilon=2 (d) epsilon=4 (d) epsilon=8 (e) epsilon = 20. However, note that for the last two values, the MECG is significantly reduced in amplitude, which causes problems in trying to calculate an approximate FECG signal. The desired result is (c) for which the epsilon value is 4.

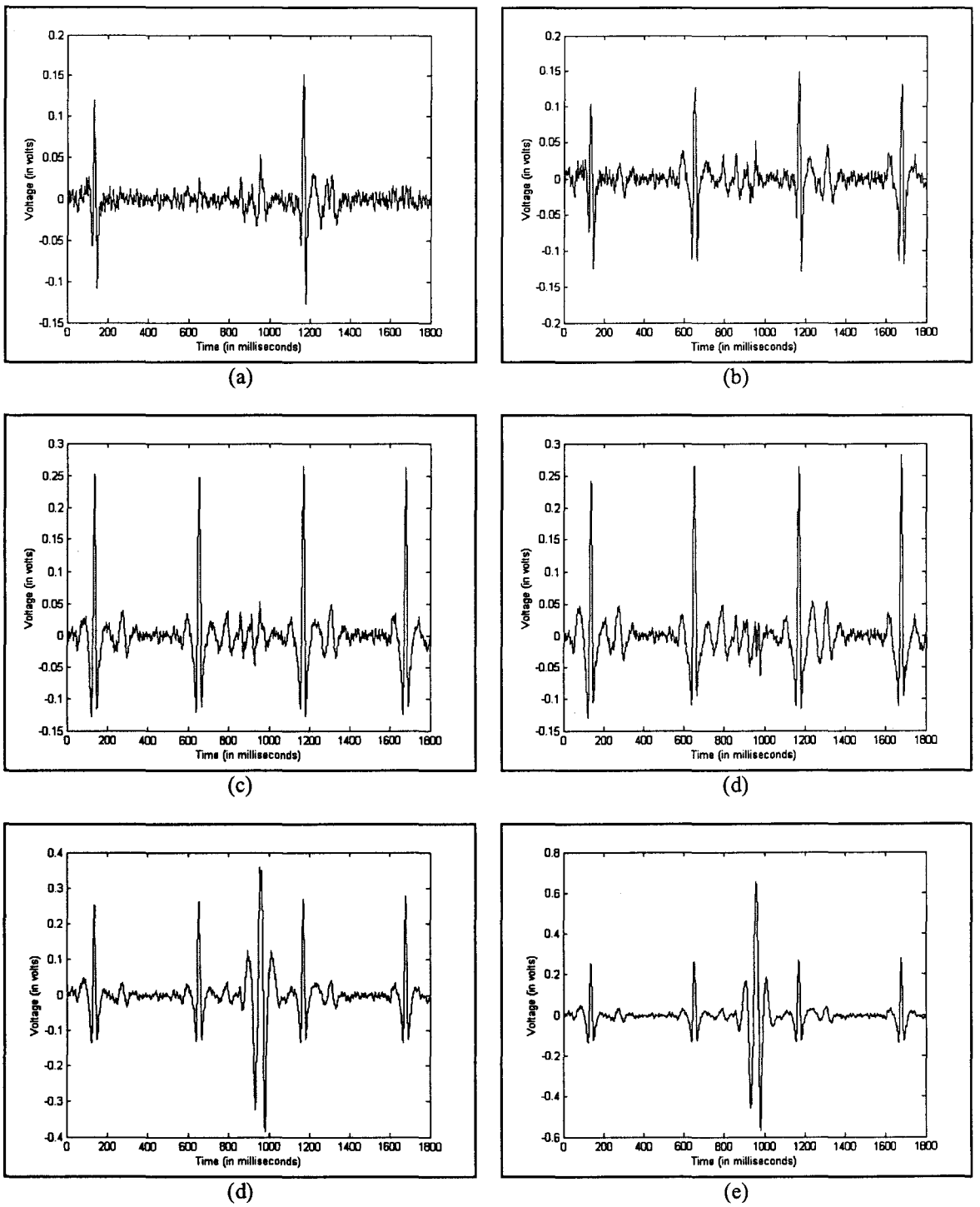

Figure 4.10 Approximate FECG signals from subtracting the processed signal from the original signal for various nearest neighbourhood radius (epsilon) values. (a) epsilon=0.5 (b) epsilon=1 (c) epsilon=2 (c) epsilon=4 (d) epsilon=8 (e) epsilon = 20. Note that the FECG waveform is incomplete in (a) because the FECG was not adequately suppressed in the previous step. In addition, the attenuation of the MECG signal in Figure 4.9d and 4.9e result in an MECG waveform in the associated FECG approximations. The ideal best result is (c), for which epsilon is 4.

required to see any noticeable "corrections" to the original signal (the actual number of delay coordinates used depended on the sampling rate). However, it was found that of all parameters, the NLNR process is least sensitive to the number of delay coordinates used. An increased number of delay coordinates only lengthen the computation time.

4.4 NLNR ON K. U. LEUVEN DATA

A similar bank of tests were performed on a data set obtained online from http://www.esat.kuleuven.ac.be/sista/daisy/ where Katholieke Universiteit Leuven in Belgium has made available the cutaneous potential recordings of a pregnant woman. This is a portion of the data used by De Lathauwer (2000) to demonstrate the effectiveness of BSS on abdominal MECG-FECG signals. Figure 4.9 displays a segment of the K. U. Leuven recording and a two-dimensional delay space representation. The data appeared to be sampled at 250 Hz and the amplitude was scaled.

4.4.1 Embedding Window Length

The embedding window length m was varied as before. The results were consistent with the results from Section 4.3. The embedding window that gave ideal results in terms of suppressed FECG and preserved MECG corresponded to the case when $m=20$ and $\tau=2$, and when $m=10$ and $\tau=2$. For a 250 Hz sampled signal is equal to an embedding window of 152 ms and 72 ms, respectively. For other values of m and τ we again have difficulty in adequately subtracting the MECG component (note the

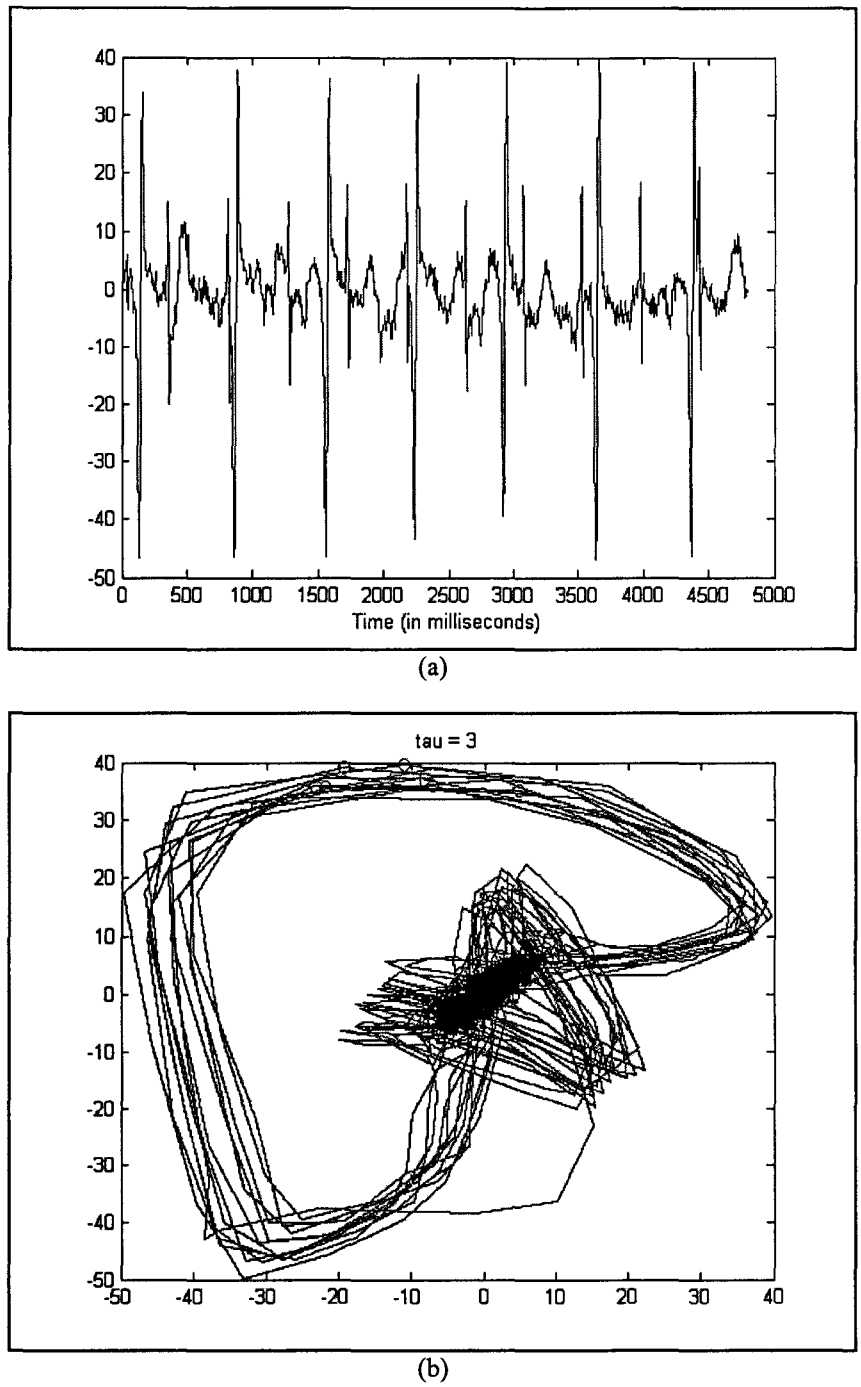

Figure 4.11 A sample of the K. U. Leuven MECG-FECG signal (a) and a two-dimensional delay-space representation for tau = 3 and m = 2 (b).

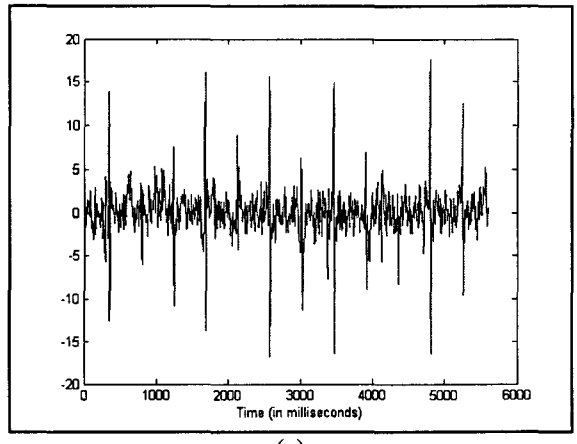

(a)

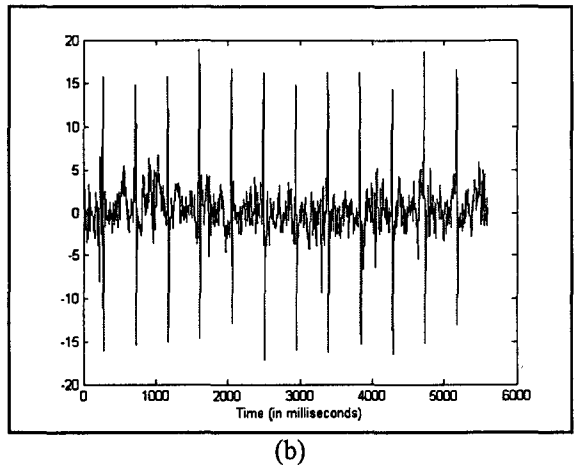

(b)

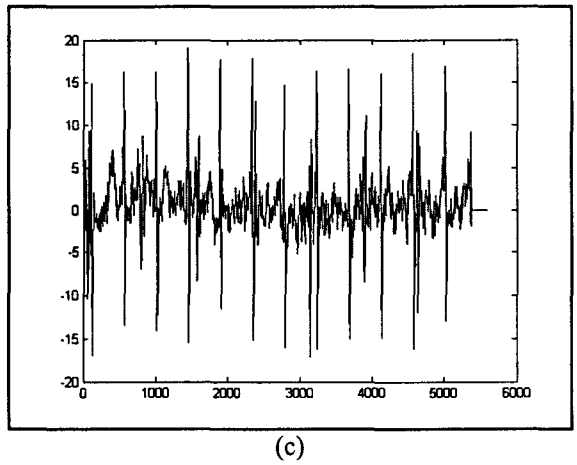

(c)

Figure 4.12 Approximate FECG signals from subtracting the processed signal from the original signal for various τ values (a) $\tau=1$ (b) $\tau=2$ (c) $\tau=4$. In the presence of noise, the embedding window size is increasingly critical in terms of adequately subtracting the MECG component and preserving the FECG component. For all three cases, *m=20* and *epsilon=15*.

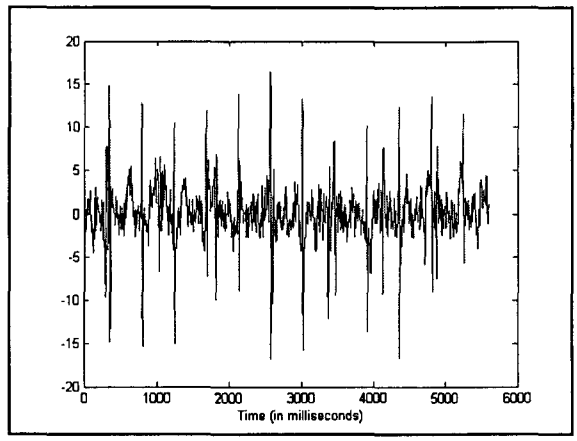

(a)

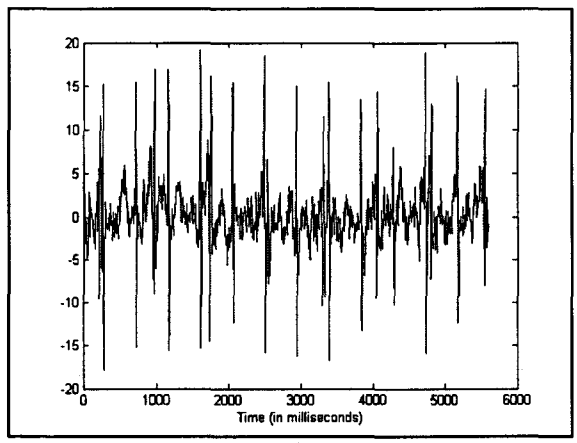

(b)

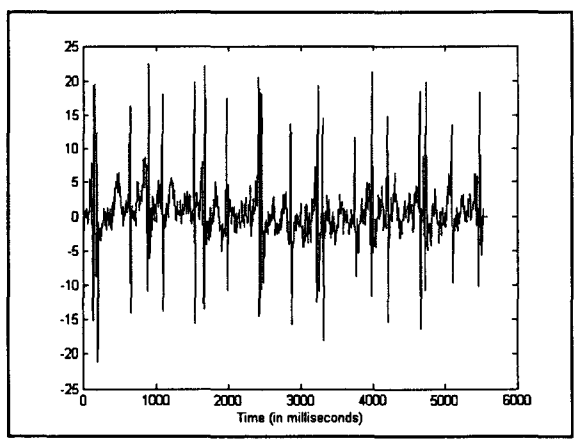

(c)

Figure 4.13 Approximate FECG signals from subtracting the processed signal from the original signal for various τ values (a) τ=*1* (b) τ=*2* (c) τ=*4*. The *epsilon* value has been increased to 25, which results in undesired residual MECG components for all three embedding window lengths.

residual MECG components in Figure 4.12c). It was difficult to extract the complete FECG signal, even for the ideal case. However, the FECG is sufficiently unambiguous for calculating the R-R intervals of the FECG and, subsequently, the fetal heart rate variability.

4.4.2 Nearest Neighbourhood

In order to isolate the FECG, we observed that the nearest neighbourhood radius falls between the maximum amplitudes of the fetal and maternal R-waves. For the K. U. Leuven data, the corresponding values are approximately 10 units and 40 units, respectively. Over a range of epsilon values between these two extremes, optimal FECG extraction occurs closer to the FECG R-wave value. Figures 4.12 shows good FECG isolation for an *epsilon* value of 15, but Figure 4.13 shows how, for the same embedding window size, an *epsilon* value of 25 results in residual MECG components in the approximated FECG signal.

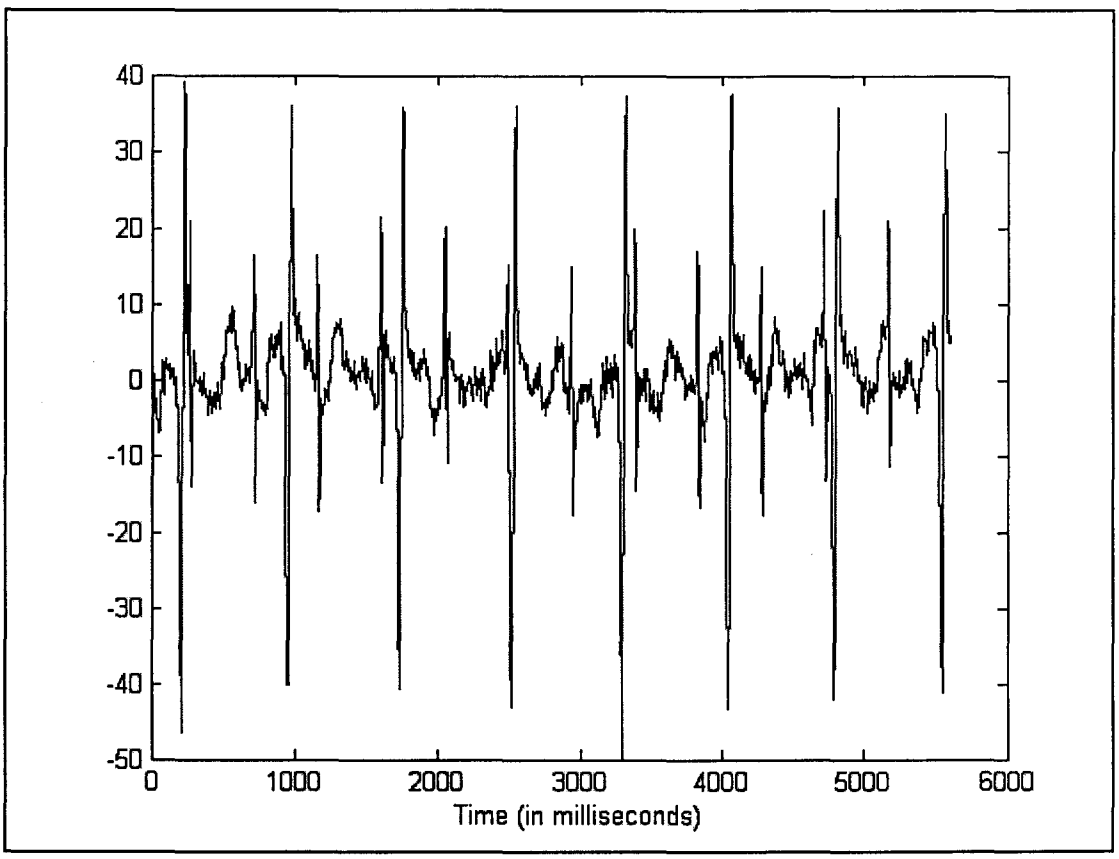

Figure 4.14 A segment of the the original K. U. Leuven signal. The "SNR" between the MECG component of the signal and the FECG component of the signal is about 10 dB.

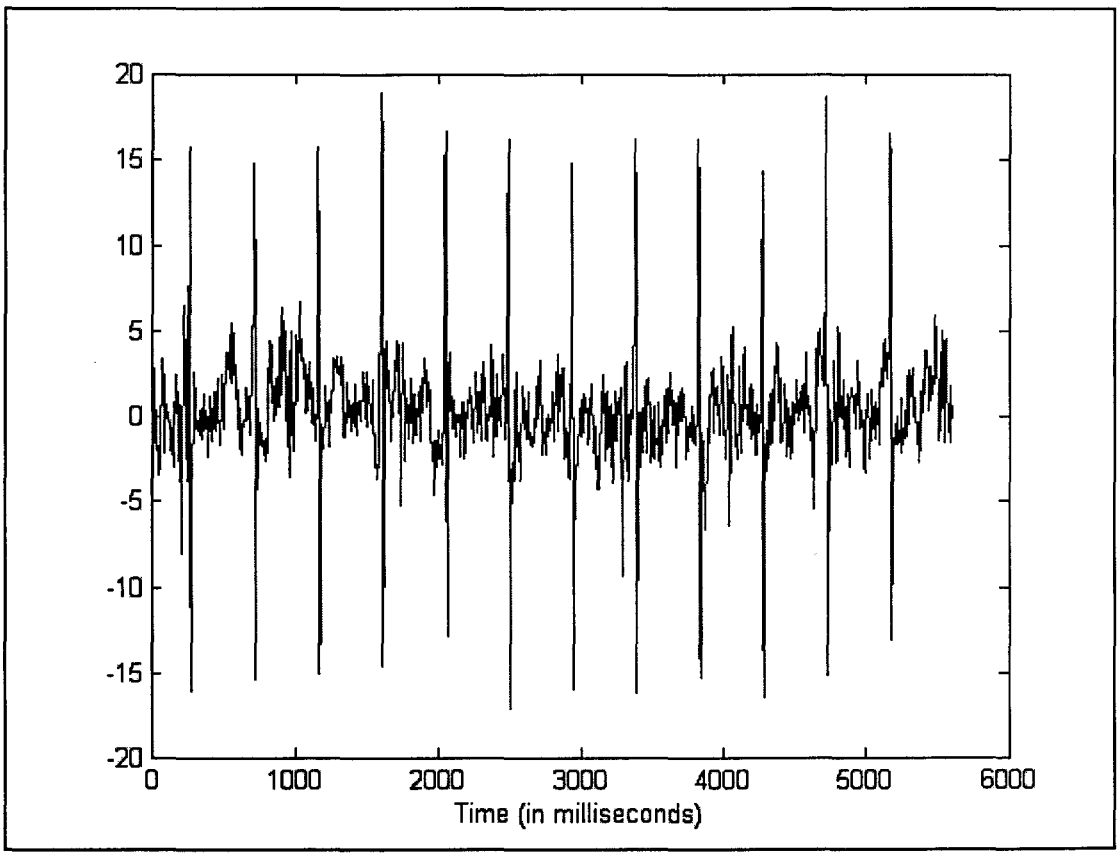

Figure 4.15 An approximate FECG signal. The extraction of the prominent R-wave allows for the straightforward calculation of derivative quantities such as the fetal heart rate.

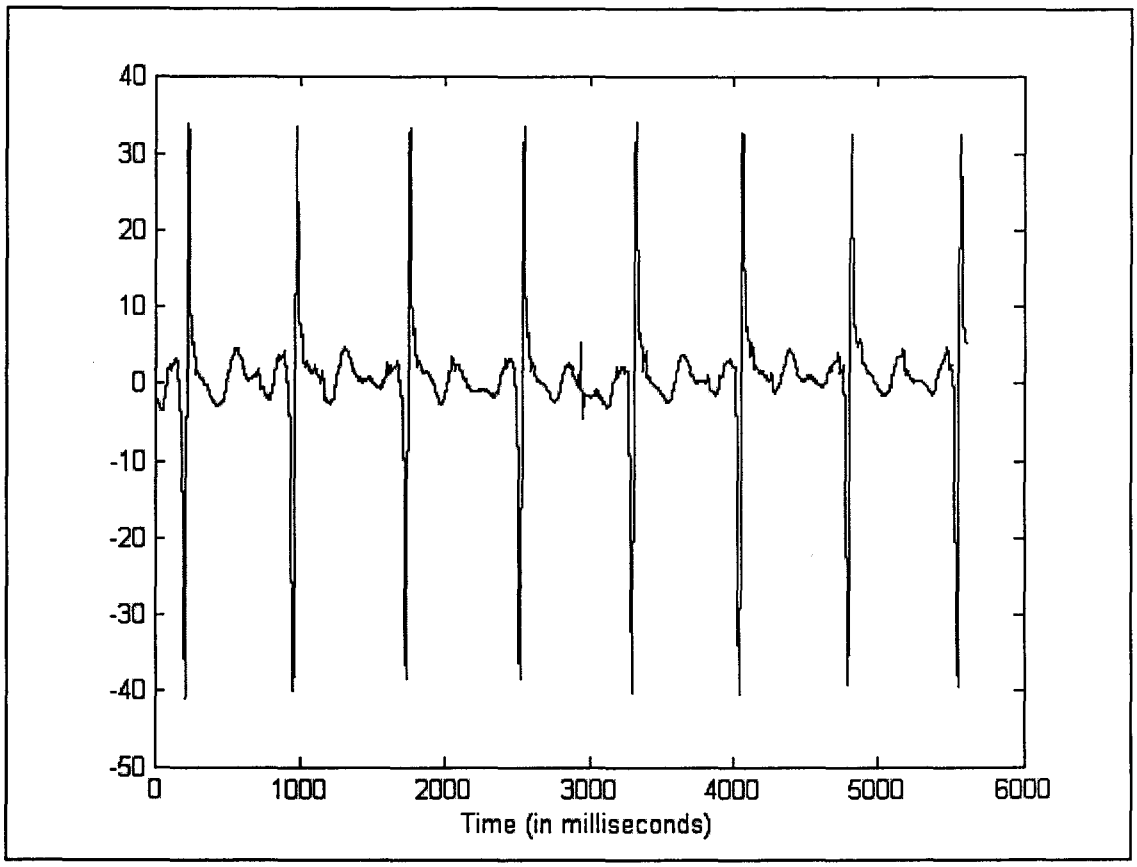

Figure 4.16 Approximate MECG signal. The NLNR process has effectively removed the fetal waveform and preserved the maternal waveforms. The better the preservation of the MECG, the more effectively it can be used to lessen the presence of a MECG component in the approximate FECG signal (see Figure 4.15).

4.5 BLIND SOURCE SEPARATION ON ABDOMINAL RECORDINGS

In the absence of any detectable FECG component, the abdominal recordings made at McMaster University Medical Center were combined with a re-sampled and scaled adult ECG that would simulate the FECG (Figure 4.5). The scaling of the adult ECG was varied to investigate the particular levels for which a BSS can successfully isolate the fetal signal. The main criterion for separation is the ability to visually discern the R-wave of the fetal signal and detect the R-wave through a QRS detection algorithm that is typically employed in heart rate variability software. The amplitude of the FECG was varied such that the SNR between the MECG and FECG defined by

$$SNR_{MF} = 20\log_{10}\frac{MECG_{RMS}}{FECG_{RMS}} \tag{4.1}$$

ranges from 12 dB to 6 dB. $MECG_{RMS}$ and $FECG_{RMS}$ are the root mean square values of a segment of the maternal and fetal signal, respectively. 12 dB roughly corresponds to the case when the maternal R-wave is about 10 times the amplitude of the fetal R-wave and 6 dB corresponds to the case when the difference is approximately a factor of 2. Recording a fetal R-wave greater than half the amplitude of the maternal R-wave is highly unlikely.

Only for one of the four recordings did the FastICA algorithm yield favourable results. For this one case, the maximum SNR_{MF} corresponding with a visible fetal signal among the separated signals was 10 dB (Figure 4.18). The noise contained within the separated FECG signal caused the peak-detection algorithm to fail, but we were able to reduce the noise by applying the NLNR process (m = 10, τ = 4, epsilon = 2.5). A segment of the resulting FECG signal is visible in Figure 4.19. In addition, we can see

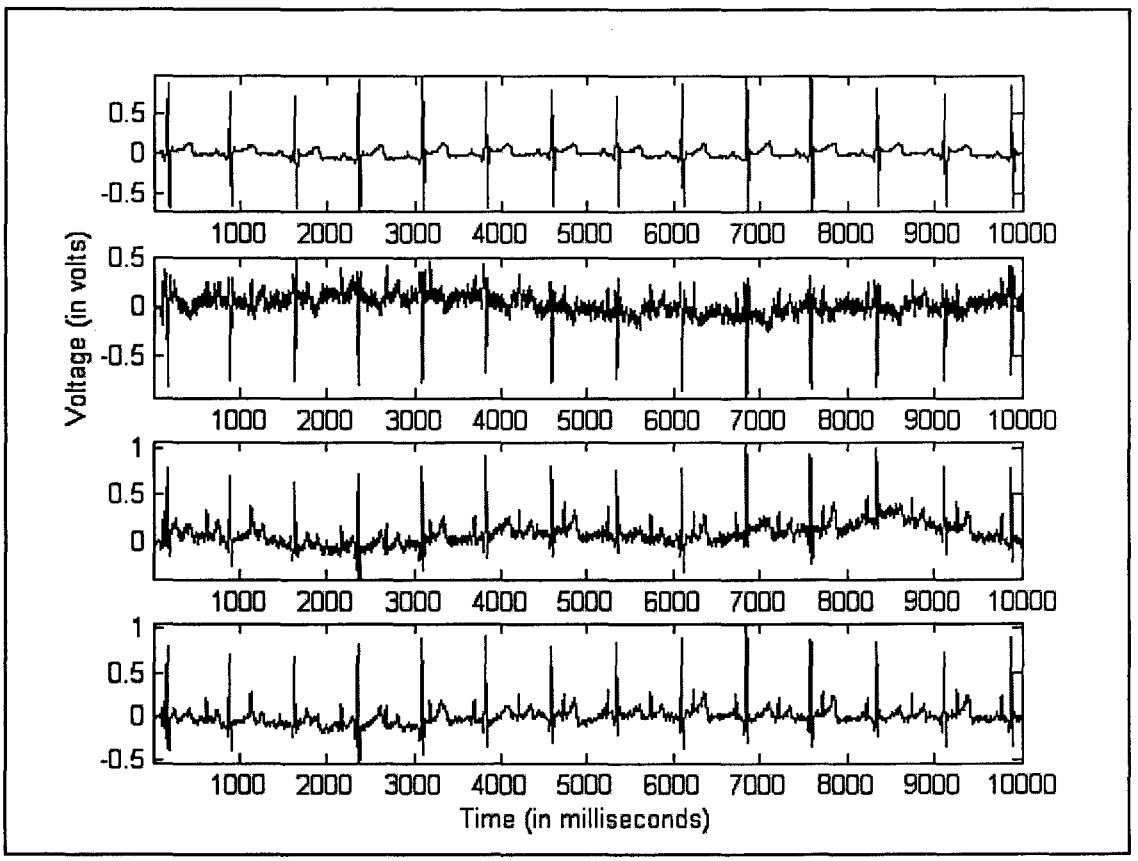

Figure 4.17 Thoracic (top) and abdominal (rows 2 to 4) recordings mixed with a scaled and re-sampled ECG signal simulating a FECG component. The signal-to-noise-ratio between the MECG and FECG components in the simulated is 10 dB.

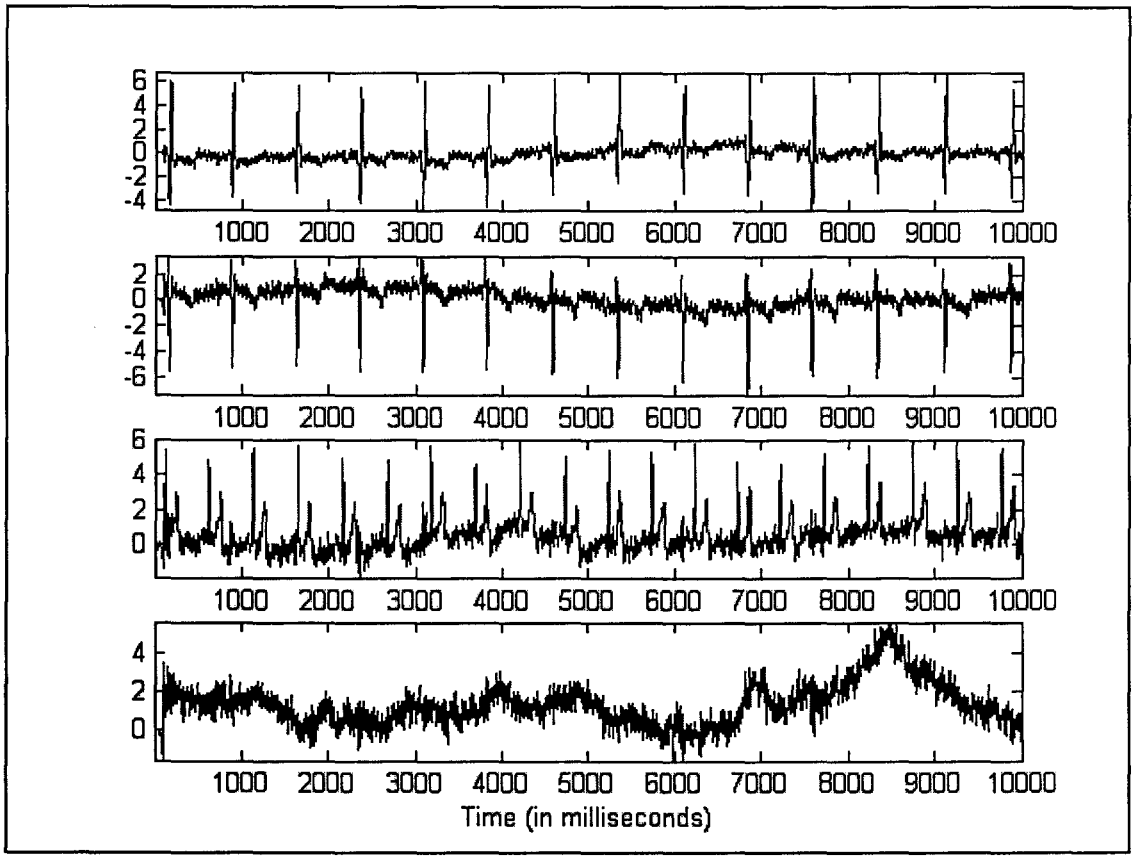

Figure 4.18 Successful separation of the fetal signal (third from top). The signal-to-noise-ratio between the MECG and FECG components in the simulated signal before the ICA algorithm was performed was 10 dB. The noise that was present is mostly concentrated in the bottom component.

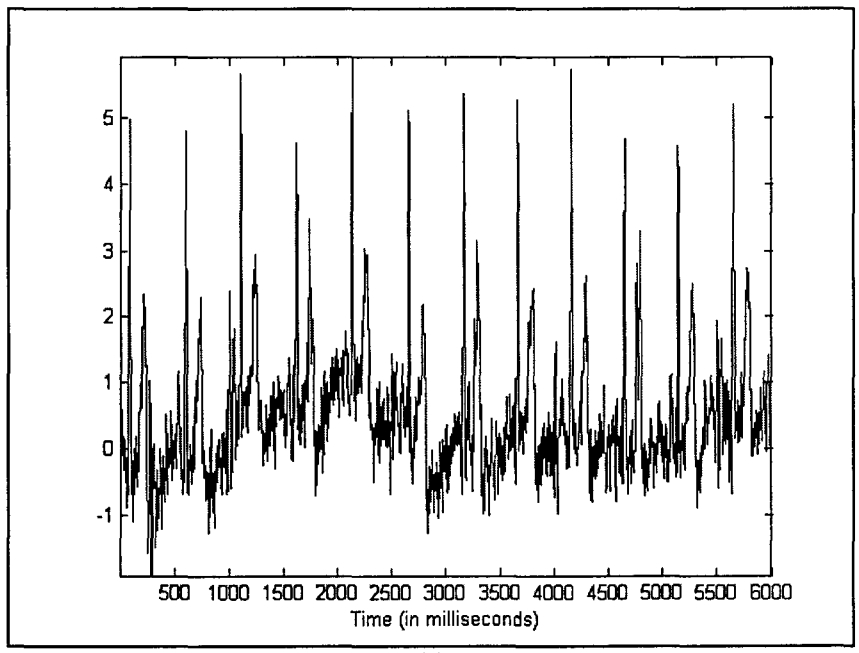

(a)

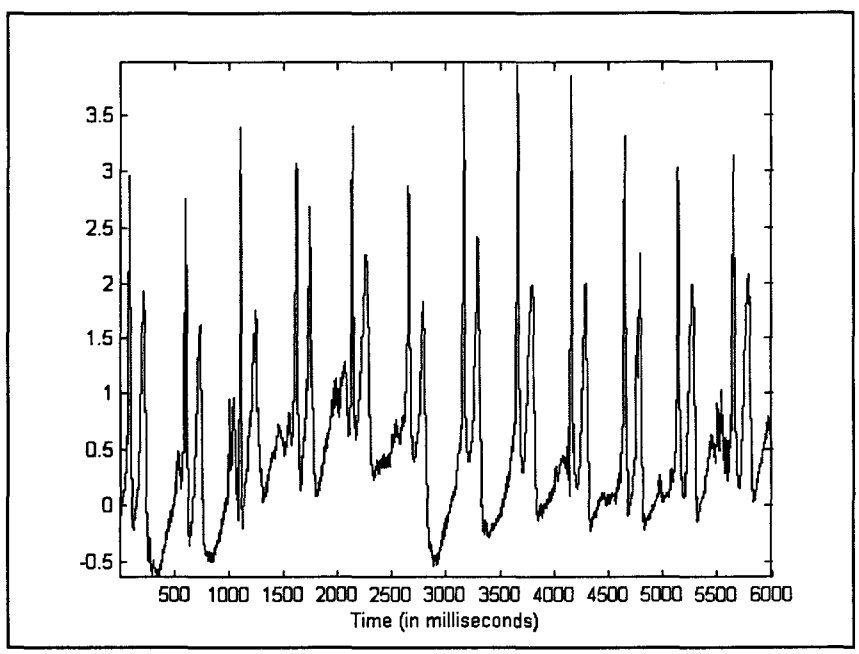

(b)

Figure 4.19 The third output component of the BSS process before (a) and after (b) an additional noise reduction process using the NLNR method (embedding window length of 72 ms and epsilon of 2.5). This will facilitate the use of an automated peak detection algorithm that fails in the presence of excess noise.

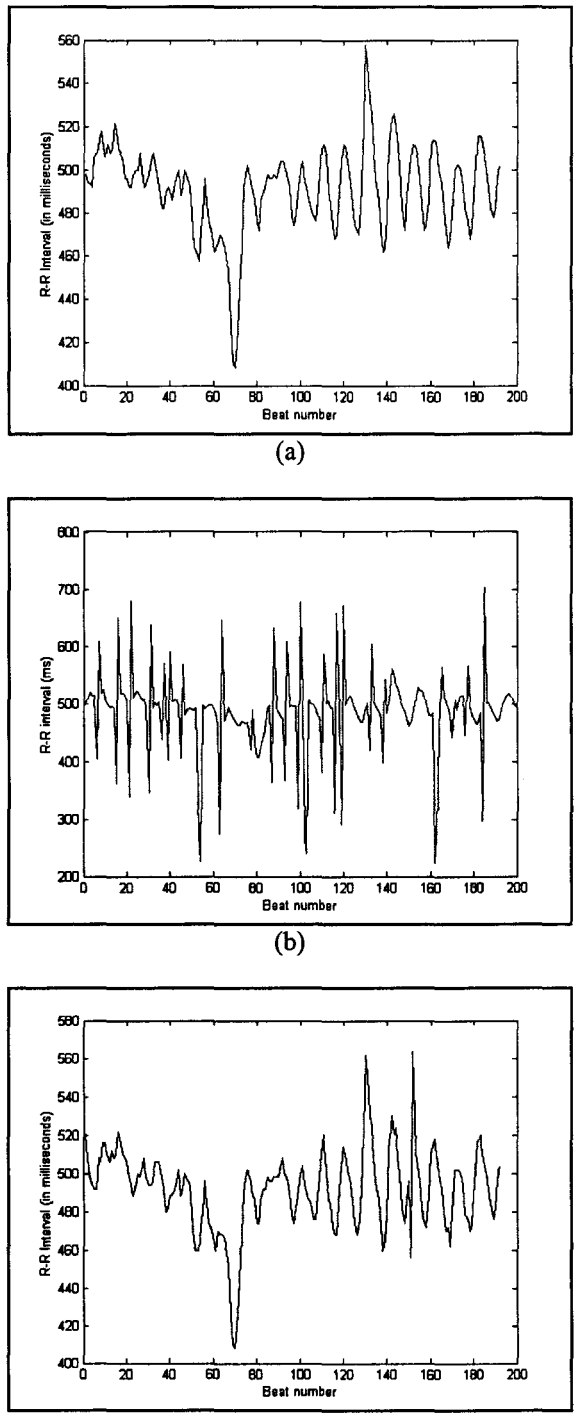

Figure 4.20 R-R intervals from the FECG signal (a) prior to being mixed into the abdominal recordings (b) the R-R intervals after extraction and (c) the R-R intervals after extraction and noise reduction. Improved QRS detection results from the noise-reduced FECG component displayed in Figure 4.19b. There error at beat 150 is due to motion artifact.

that an application of NLNR significantly improves the detectability of the R-wave using our QRS detection algorithm (Figure 4.20). The remaining three recordings processed using the FastICA algorithm did not yield favourable results, but gave insight into the limitations of ICA as a scheme to isolate the fetal component. The primary difficulty when using BSS to generate an approximate FECG signal lies in keeping the number of extraneous signals equal to or less than the number of recording channels. Recordings from three patients that did not result in a clean FECG signal using ICA at an $SNR_{MF} = 6$ dB all contained various combinations of line noise, motion artifacts, and baseline wander. Motion artifacts often appeared unpredictably across channels. Thus, we can interpret the difficulty in extracting the fetal ECG as a case of too many sources and an insufficient number of observations. In addition, motion artifacts and baseline wander cause the distributions of recorded signals to be highly nonstationary. Since ICA is dependent on estimating various probability distributions of the embedded signals, these factors also make source separation increasingly challenging.

We thus see that although $SNR_{MF} = 10$ dB is sufficient for extracting the FECG, the success of the extraction is dependent on the extent of noise suppression that has been performed beforehand as well as the number of available channels.

4.6 SUMMARY

Our results demonstrate that the NLNR technique is capable of separating the FECG R-wave from a mixed signal both for synthetic mixed signals and real abdominal recordings. We determined that the embedding window length needs to be roughly a tenth of the size of a typical adult ECG R-R interval or approximately 100 ms. The

nearest neighbourhood radius yields optimal separation for a value greater than the R-wave amplitude of the fetal signal, but significantly less than the maternal R-wave amplitude.

Blind source separation is capable of extracting the FECG under low noise conditions. The resulting ECG is visually easily recognizable and can be processed using an automated QRS detection algorithm with good results. However, in the presence of motion artifacts, 4-channel ECG is insufficient to adequately extract a sufficient quantity of the fetal component.

Chapter 5

Discussion and Recommendations

5.1 COMPARISON OF TECHNIQUES

Both the nonlinear noise reduction and blind source separation techniques aid in the extraction of the FECG. The most conspicuous similarity between the two techniques is their sensitivity to low-frequency noise. Motion artifacts are to be minimized and/or eliminated completely in a preprocessing stage through linear filtering. In the absence of such noise, and with a minimum of 4 channels, the blind source separation (BSS) method can extract an FECG signal for an SNR_{MF} of approximately 10 dB. Although the NLNR technique works with a slightly lower SNR_{MF}, the quality of the resulting FECG signal is not any different. With an additional noise reduction step following the FECG extraction process, (for either method) the final FECG signal is such that it lends itself to automated QRS detection.

In terms of performance, the nearest neighbourhood search slows down the NLNR algorithm considerably. The time-consuming nature of finding optimal parameter values is partly resolved by using the results in Section 4.4 as a guide. Determining the ideal parameters could perhaps be quickened through the use of visual feedback of the effects of parameter changes. This is in direct contrast to FastICA algorithm which has fewer parameters to optimize although it is consequently less intuitive to modify. The positive and negative aspects of each technique are summarized in Table 5.1.

	Advantages	**Disadvantages**
Nonlinear Noise Reduction	- Only a single channel of mixed ECG is necessary - Common framework for both FECG extraction and noise reduction - Can obtain an MECG only signal whose amplitude matches the MECG component of the original mixed signal	- Computationally expensive due to nearest neighbour search required on every iteration - Sensitive to low-frequency noise - Requires "fine-tuning" of parameters
Blind Source Separation	- Fast convergence - Given a sufficient channels, noise can be separated as a component	- Separation is difficult in the presence of several noise sources

Table 5.1 Comparison chart of NLNR and BSS with respect to FECG extraction.

5.2 RECOMMENDATIONS AND FUTURE CONSIDERATIONS

The results of the recordings and experiments done during the course of this thesis indicate that the necessary signal processing technology is available to sufficiently isolate the fetal signal from a mixed MECG-FECG signal to assess indicators of fetal health such as the fetal heart rate. One area that will require attention in the future is the recording process. Two things in particular need to be explored: A consistent and reliable protocol for the placement of electrodes and increased common mode rejection (CMRR) by the amplifiers. Until both of these issues are resolved, signal-processing techniques employed to isolate the fetal ECG component will remain inadequate for timely clinical use.

We are still in the initial stages of systematically obtaining optimal electrode location and very little literature exists that documents a consistent framework for abdominal recordings. We need to establish the optimal stage of pregnancy for abdominal recordings, which according to Dr. Patrick Mohide of McMaster University Medical Center is around 26 to 27 weeks. In addition to further consultation with physicians about possible factors that would aid in efficiently recording fetal signals from abdominal electrodes, we need to conduct multiple electrode "mapping" sessions (multichannel recordings over a grid on the maternal torso) that would deepen our knowledge of how the fetal signal traverses its way through maternal tissue to various points on the torso.

We have found that no fetal signal can be detected using neonatal ECG amplifiers with CMRR's of 100 dB. Although we cannot directly attribute such failure to detect a signal to the insufficiency of the instrumentation, it is reasonable to construct and employ

ECG amplifiers with CMRR close to 120 dB in our studies. In addition to improving the ability of the amplifiers to reject common signals such as 60 Hz noise, construction of custom ECG amplifiers will allow us to reduce the size of our instrumentation. For similar reasons, we recommend employing a portable computer in lieu of the current desktop model. The portability of the equipment will also facilitate maintenance and equipment modifications by eliminating the need to transport heavy equipment to and from the recording site.

Chapter 6

Summary

6.1 SUMMARY

The work described in this thesis discusses the clinical significance of the fetal electrocardiogram and current signal processing methods that can be employed to extract the fetal ECG. Chapter 1 outlines the physiological interpretations of the fetal electrocardiogram and the fetal heart rate as well as their relevance in diagnosing fetal health.

The theory underlying two recently proposed methods of FECG extraction using nonlinear noise reduction and blind source separation are outlined in Chapter 2. We discuss how nonlinear noise reduction works to transform a mixed MECG-FECG signal into an approximate MECG signal, which we can subtract from the original signal to obtain an approximate FECG signal. Blind source separation is related to the idea of

linearly combining multiple signals using a weighting matrix. The recombined signals are meant to be as statistically independent as possible, according to criteria based on higher-order statistics such as the fourth-order cumulants and related quantities such as negentropy.

In Chapter 3, we examined at the recording apparatus and the protocol used to perform abdominal recordings at McMaster University Medical Center. We identified some of the issues that were brought to our attention over the course of our research, including the difficulties in finding the optimum locations for our skin electrodes, the challenge of reducing the level of line noise in the recording space, and exploring the limitations of the existing hardware (e.g. ECG amplifiers).

Our results presented in Chapter 4 show how the NLNR process is effective in extracting the FECG signal while simultaneously suppressing noise and MECG signal content. For a mixed MECG-FECG signal, we found that an embedding window length was 90 ms and a nearest neighbourhood radius that was slightly larger than the fetal R-wave amplitude was adequate to separate the MECG signal from the FECG signal. We showed that the BSS technique could extract the FECG signal, given 4 channels of ECG data when motion artifacts and other noise components were kept at a minimum during the recording. In addition, the extracted signal's noise content was reduced by applying the NLNR process whose embedding window length and nearest neighbourhood radius was set to 72 ms and 2.5, respectively. The FECG R-wave could be easily recognized and lent itself to automated QRS detection.

Bibliography

Barcroft J (1947), Blackwell Scientific Publications: Researches on Prenatal Life, pp. 79, Oxford Publications, London.

Bemmel JHV (1966), "Two Methods for Optimal MECG Elimination and FECG Detection from Skin Electrode Signals", *IEEE Transactions on Biomedical Engineering*, 34(3): 17-23.

Bergveld P, Meijer WJH (1981), "A New Technique for the Suppression of the MECG", *IEEE Transactions on Biomedical Engineering*, 28(4): 348-354.

Blair E, Stanley FJ (1998), "Intrapartum Asphyxia: A Rare Cause of Cerebral Palsy", *Journal of Pediatrics*, 112: 515-519.

Callaerts D, De Moor B, Vandewalle J, Sansen W (1990), "Comparison of SVD Methods to Extract the Foetal Electrocardiogram from Cutaneous Electrode Signals", *Medical and Biological Engineering and Computing*, 28: 217-224.

Cardoso JF (1998), "Blind Source Separation: Statistical Principles", *Proceedings of the IEEE*, 9(10): 2005-2009.

Cover TM, Thomas JA (1991), Elements of Information Theory, pp. 242, John Wiley and Sons, New York, USA.

Crowe J (1996), "Antenatal Assessment Using the FECG Obtained Via Abdominal Electrodes", *Journal of Perinatal Medicine*, 24: 43-53.

De Lathauwer L, De Moor B, Vanderwalle J (2000), "Fetal Electrocardiogram Extraction by Blind Source Subspace Separation", *IEEE Transactions on Biomedical Engineering*, 47(5): 567-572.

Ferrara ER, Widrow B (1982), "Fetal Electrocardiogram Enhancement by Time Sequenced Adaptive Filtering", *IEEE Transactions on Biomedical Engineering*, 29(6): 458-459.

Freeman RK, Garite TJ, Nageotte MP (1991), Fetal Heart Rate Monitoring, 2nd Edition, Williams Wilkins, Baltimore Maryland, USA.

Goddard BA, Newell JA, Edwards RL, Farr RF (1966), "A Clinical Foetal Electrocardiograph", *Medical and Biological Engineering*, Pergamon Press, 4: 159-167.

Goldberger AL, Goldberger E (1997), Clinical Electrocardiography, Mosby, St. Louis, USA.

Grasberger P, Hegger R, Kantz H, Schaffrath C, Screiber T (1993), "On Noise Reduction Methods for Chaotic Data", *Chaos*, 3(2): 127-140.

Hamilton E (1996), "Fetal Health Surveillance: What Works and What Does Not", Technical Report, LMS Medical Systems Limited.

Hon EH, Lee ST (1963), "The Fetal Electrocardiogram 1 – The Electrocardiogram of the Dying Fetus", *American Journal of Obstetrics and Gynecology*, 87: 804-813.

Hyvarinen A (2000), "Fast and Robust Fixed-Point Algorithms for Independent Component Analysis", *IEEE Transactions on Neural Networks*, 10(3): 626-634.

Hyvarinen A, Karhunen J, Oja E (2000), "Independent Component Analysis: Algorithms and Applications", *Neural Networks*, 13(4-5): 411-430, 2000.

Hyvarinen A, Karhunen J, Oja E (2001), Independent Component Analysis, John Wiley and Sons, New York, USA.

Kanjilal PP, Palit S, Saha G (1997), "Fetal ECG Extraction from Single-Channel Maternal ECG Using Singular Value Decomposition", *IEEE Transactions on Biomedical Engineering*, 44(1): 51-59.

Longini RL, Reichert TA, Cho J, Crowley JS (1977), "Near Orthogonal Basis Functions: A Real Time Fetal ECG Technique", *IEEE Transactions on Biomedical Engineering*, 24: 29-43.

Luenberger DG (1969), Optimization by Vector Space Models, John Wiley and Sons, New York, USA.

Murray HG (1986), "The Fetal Electrocardiogram: Current Clinical Developments in Nottingham", *Journal of Perinatal Medicine*, 14(6): 399-404.

Pardi G, Crosignani PG (1971), "Electrocardiographic Patterns and Cardiovascular Performance of the Sheep Fetus During Hypoxia", in Pardi G, Crosignani PG, Ed., Fetal Evaluation During Pregnancy and Labour, pp. 157-174, Academic Press, London.

Richter M, Schreiber T, Kaplan DT (1998), "Fetal ECG Extraction with Nonlinear State Space Projections", *IEEE Transactions on Biomedical Engineering*, 45(1): 133-137.

Schreiber T, Kaplan DT (1996), "Nonlinear Noise Reduction for Electrocardiograms", *Chaos*, 6(1): 87-92.

Schreiber T, Kaplan DT (1996), "Signal Separation by Nonlinear Projections: The Fetal Electrocardiogram", *Physical Review E.*, 53: R4326-R4329.

Siassi B (1973), "The Effect of Arterial p02 in the Cardiovascular Response to Umbilical Cord Compression", Presented at the 20th Annual Meeting of the Society for Gynecological Investigation, Atlanta, Georgia, USA.

Southern EM (1957), "Fetal Anoxia and its Possible Relation to Changes in the Prenatal Fetal Electrocardiogram", *American Journal of Obstetrics and Gynecology*, 73: 233.

Sureau C (1955), "Etude de l'Activite electrique de l'Uterus au Cours de la Gestation et du Travail", Thesis, Faculty of Medecin, Paris, France.

Symmonds EM, Sahota D, Chang A (2001), Fetal Electrocardiogrpahy, Imperial College Press, London.

Wheeler T, Murrillis A, Shelly T (1978), "Measurement of the Fetal Heart Rate During Pregnancy by a New Electrocardiographic Technique", *British Journal of Obstetrics and Gynecology*, 85: 12-17.

Vanderschoot J, Callaerts D, Sansen W, Vandewalle J, Vantrappen G, Janssens J (1987), "Two Methods For Optimal MECG Elimination and FECG Detection from Skin Electrode Signals", IEEE Transactions on Biomedical Engineering, 34(3): 233-243

Zarzoso V, Nandi AK (2001), "Noninvasive Fetal Electrocardiogram Extraction: Blind Separation Versus Adaptive Noise Cancellation", *IEEE Transactions on Biomedical Engineering*, 48(1): 12-18